University of Stavanger

Faculty of Science and Technology

MASTER'S THESIS

Study program/ Specialization: Petroleum Engineering / Drilling	Spring semester, 2015 Open
Writer: Jieyin Liu	…… (Writer's signature)
Faculty supervisor: Dan Sui External supervisor(s):	
Thesis title: **Automatic MPD & Downhole temperature estimation and temperature effect on density**	
Credits (ECTS): 30	
Key words: Downhole temperature behavior; Predict density behavior under isobaric condition; Temperature and pressure effect on density; BPP method in automatic MPD	Pages: 84 + enclosure: 6 Stavanger 15-June-2015 Date/year

Preface

This thesis concludes my Master of Science degree at the department of Petroleum engineering at the University of Stavanger in Norway, during the spring term 2015.

Everything from scratch is not an exaggeration when I started to simulate in MATLAB. I met many difficulties along the way. In order to make the results at a reasonable level, a lot of effort has been put into simulations. Fortunately, it became joyful at the end.

I would like to thank my parents for letting me know the importance of education.

I am indebted to my husband Ingve and our children for supporting me through such many years, which made my Master's degree possible.

Special thanks to my friend Daniel Pippin for spending his time on going through this thesis.

The author is grateful to Mesfin Agonafir Belayneh for his kindness in giving the motivation to carry on the thesis when I needed.

I also would like to thank Kjell kåre Fjelde and Tom Ryen for their helpful suggestions in MATLAB. Additional comments and encouragements by friends and fellows are appreciated.

Abstract

Hydraulic model is the ‘brain’ of an automated managed pressure drilling (MPD) control system. It requires knowledgeable people to set up and tune before operation starts.

Glenn-Ole Kaasa’s simplified dynamic wellbore model has been often utilized in recent years. It is able to model fluid flow during drilling under the condition of uniform flow pattern in the drillstring and annulus along the complete length. In this study, on the basis of the Kaasa’s model, a simulation of backpressure pump (BPP) method was given for the purpose of demonstrating automatic pressure control during a drillpipe connection process.

A primary challenge during drilling high temperature and high pressure (HTHP) wells is to maintain a constant bottom hole pressure (BHP) in a relatively narrow operating window. Temperature plays a very important role on density determination. A small change in density can cause great pressure fluctuation in BHP.

In this study, the downhole temperature behaviors are predicted for a circulating well on the basis of Eirik Kaarstad’ work[1], then couples this temperature model into a linearized density equation in order to study the downhole density under isobaric condition. The model is valid for using of incompressible drilling fluid. It assumes steady-state heat transfer in the wellbore and transient heat transfer in the formation.

A large number of sensitivity analysis are performed in this study based on the temperature and density model. The results provided by these comparisons show how those different variables with variety of values can influence the temperature and density behaviors under circulation condition and moreover to what extent the temperature and density were affected. It gives a very good picture of dynamic downhole temperature and density behaviors.

Table of Contents

List of figures

List of tables

Nomenclature

List of symbols

P_{pore} = Pore Pressure

$P_{bottomhole}$ = Bottom Hole Pressure

$P_{wellbore\ stability}$ = Wellbore Stability Pressure

$P_{fracture}$ = Fracture Pressure

$P_{downhole}$ = Downhole Pressure

P_{static} = Hydrostatic Pressure

P_{dyn} = Hydrodynamic Pressure

P_{back} = Back-Pressure

P_{dh}^{ref} = Downhole Reference Pressure

P_{dh} = Downhole Pressure

U = Overall Heat-Transfer Coefficient

List of abbreviations

HTHP = High Temperature, High Pressure

MPD = Managed Pressure Drilling

BHP = Bottom Hole Pressure

BPP = Back Pressure Pump

RPD = Rig-Pump Diverter

NPT = Non-Productive Time

ECD = Equivalent Circulating Density

UBD = Underbalanced Drilling

OBD = Overbalanced Drilling

RCD = Rotating Control Device

BOP = Blow Out Prevent

NRV = Non Return Valves

CBHP = Constant Bottom Hole Pressure

DGD = Dual Gradient Drilling

PID = Proportional, Integral and Derivative Controller

ROP = Rate of Penetration

HSE = Health, Safety and Environment

MWD = Measurement While Drilling

PLC = Programmable-Logic Controller

ESD = Equivalent Static Density

PVT = Pressure/Volume/Temperature

1 Introduction

As the oil industry does not look quite optimistic nowadays, emphasis is placed on increasing automation development.

Automatic MPD with a fluid hydraulic model automatically calculating how much additional surface backpressure need to be applied when bottom hole pressure (BHP) changes. The automatic choke system rapidly and timely close or open the choke in order to enable control of the annulus downhole pressure and maintain the BHP at a constant level above the pore pressure and below the fracture formation pressure.[18]

Automation in drilling improves well control, thereby increasing safety for personnel. As automated operation requires no human control on the drilling operation.

Density of drilling fluid depends on the expansion or contraction of the fluid. Fluid expands due to increasing temperature while it shrinks due to increasing pressure. In shallow wells compressibility and thermal expansion have not much influence on density, however in deepwater and high temperature and high pressure (HTHP) environment they become significant since the temperature and pressure vary over a broad range. [14]

MPD technology is often the first option suggested in those challenging wells due to narrow safe margins between pore pressure and the formation fracture pressure. A restricted operating window means almost no room for error when estimating BHP. This tight operation window requires reliable information of downhole temperature and annular pressure profiles to enable adjusting of surface choke position and applying of surface backpressure for maintaining stable BHP in order to avoid well control problems and formation damages. [19]

Especially, when measured data only provides limited information for interpreting of the downhole situation, then an available temperature profile can provide better understanding of the downhole situation for drillers and the rest of the rig crew. Thereby ensuring a successfully MPD drilling operation.

1.1 Scope and objective

This thesis is divided into 7 sections and it including three main parts:

- MPD drilling technology (Section 2 and 5)
- Temperature model (Section 6)
- Case studies:
  Case 1: Predicting of downhole temperature and density behavior (Section 7)

  Case 2: Simulation of backpressure pump (BPP) method in automatic MPD (Section 7)

The MPD drilling technology sections are intended to describe the manual MPD technology and automated MPD. A comparison of backpressure pump (BPP) MPD and rig pump diverter (RPD) MPD were briefly described.

A brief overview of a temperature model was given in section 6. It is based on the book by Eirik Kårstad, for the purpose of predicting downhole temperature.

The objective of case 1 was to first apply the temperature model to predict the annular and drillpipe temperature behavior under forward circulation condition. Next, using this temperature model coupled with a density model for determining the downhole density behavior under isobaric condition. In the case study, by selecting *circulation rate; circulation time; heat capacity; geometry; inlet mud temperature* and *overall heat coefficient* as six input variables in the simulation, the temperature and density results with different values of unlike variables are compared and highlighted. It has attempted to keep the simulation result at a reasonably level, thus unlike values of different variables are carefully selected.

The main purpose of case 2 was to simulate a jointed pipe connection in order to show the performance of backpressure pump (BPP) method in automatic MPD technology and the results have been briefly discussed.

MATLAB was utilized as the simulation tool for both case studies.

2 MPD drilling technology

2.1 Introduction

MPD technology has developed on land for decades and hugely driven the oil and gas industry forward. The methodology is gaining in popularity offshore and becomes a prior selection for drilling wells with high drilling risk that otherwise might be un-drillable and economically uncompetitive with conventional drilling concept. In addition, when drilling with conventional overbalanced method, an amount of unnecessary non-productive time (NPT) has to spend on solving classic problems such as kicks, lost circulation and stuck pipe. In hostile marine environment in particularly deep wells and ultra-deep wells, they are technical and economically challenging to develop, even though, by proper selection of MPD technique, well-planning and skillful project engineering, the MPD technology have led to various operators and service companies benefitted from many drilling operations.[20] [21]

MPD drilling technology is presented in this section. It gives an overview of the following topics:

- Variations of MPD
- Equipment related to MPD
- Main benefits of MPD

2.2 Why use managed pressure drilling (MPD)?

Drilling using conventional method in deep water, depleted formation, extended reach wells and HPHT are challenging, and the main reason is narrow operation window between formation pore pressure and fracture pressure. If well pressure is lower than the formation pressure, influx of formation fluid may occur and a potential kick situation is underway, in worst scenario, a blow-out event happens. On the other hand, if well pressure is higher than formation pressure, it can cause damage of formation near the borehole and mud losses, it can be costly. A small change in the bottom hole pressure situation can result in possibly fluid losses or gas kick when operates within a small operation window, further in turn increased non-productive time (NPT). Application of MPD is a solution. MPD provide benefits in a wide range of applications. [2]

Managed pressure drilling is frequently applied to obtain some specific purposes such as reduce number of casing strings, prevent formation damage in a specific section in a well.

With the primary objective of maintaining a constant bottomhole pressure, MPD technology has advanced equipment allows it solves problems such as drilling through tight pressure windows and reduce of equivalent circulating density (ECD) in extended reach wells.[21]

Fig.1 illustrates the criterion for UBD where bottomhole pressure (BHP) is lower than pore pressure but higher than wellbore stability pressure. The relationship can be expressed like this:$P_{pore} > P_{bottomhole} > P_{wellbore\ stability}$, and criterion for OBD is described as BHP stays higher than pore pressure and under formation fracture pressure. The relationship can be written as : $P_{pore} < P_{bottomhole} < P_{fracture}$. [2]

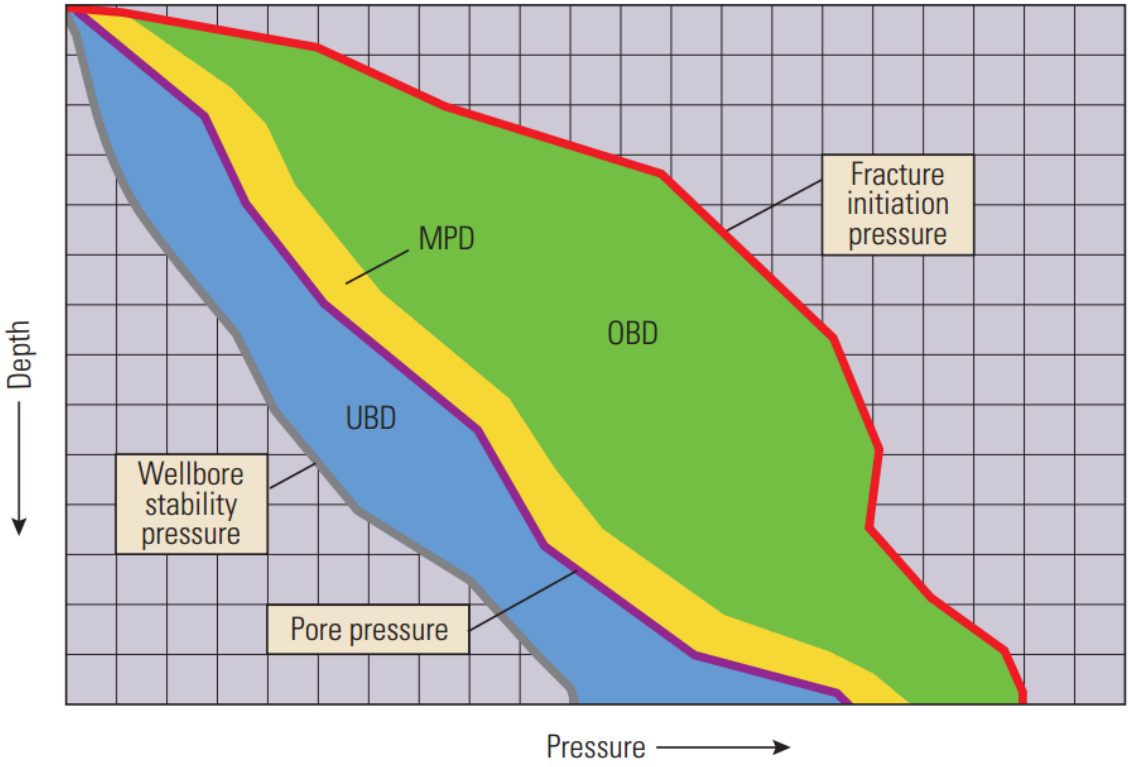

Figure1: An illustration of the drilling windows for conventional or overbalanced drilling (OBD), underbalanced drilling(UBD) and managed pressure drilling(MPD).[2]

2.3 Underbalanced drilling method

UBD is a technique in which the pressure in the wellbore is maintained lower than the reservoir pressure to prevent loss to the formation while drilling a well. UBD condition is often created artificially by injection of less-dense gas to the liquid phase of the drilling fluid. Nitrogen is most commonly used. This condition invites reservoir fluids flow into the wellbore to reduce invasive formation damages, on the other hand, the increased penetration rate that created by greater weight on bit can also lead to reduction in drilling time.[22]

2.4 MPD vs UBD

MPD and UBD have mange aspects in common based on the required surface equipment. However, MPD is distinguished from UBD since MPD addresses drilling-related problems that lead to non-productive time (NPT) such as differential sticking, blowouts. It improves drilling processes and reduce NPT by minimizing wellbore breathing. While UBD solves mostly reservoir-related challenges and thereby improve reservoir performance. Furthermore, UBD

provide distinctive well testing conditions to define properties of reservoir layer while drilling.[20] [23]

2.5 Theory of managed pressure drilling (MPD)

With conventional drilling concept, the downhole pressure ($P_{downhole}$) contains two parts:

1. The hydrostatic pressure of the mud column including cuttings (P_{static}). Commonly note as mud weight (MW).
2. The hydrodynamic pressure in the annulus induced by various effects from drilling fluid flowing or drill pipe rotation (P_{dyn}). This is often referred as annular friction pressure. The effect of these two parts is given by the following relationship:

$P_{downhole} = P_{static} + P_{dyn}$ [24]

$P_{static} = \rho * g * h$

$P_{dyn} = \frac{f_D * \rho * v^2}{d} * h$

$f_D = \frac{64}{R_e}$

Where

$\rho = density\ of\ drilling\ fluid$

$g = gravity$

$h = height\ of\ mud\ column$

$f_D = Darcy\ friction\ factor$

$v = velocity$

$d = hydraulic\ diameter$

$R_e = Reynolds\ number$ [11]

Fig. 2 shows Pressure vs Depth, Downhole pressure static VS Downhole pressure dynamic.

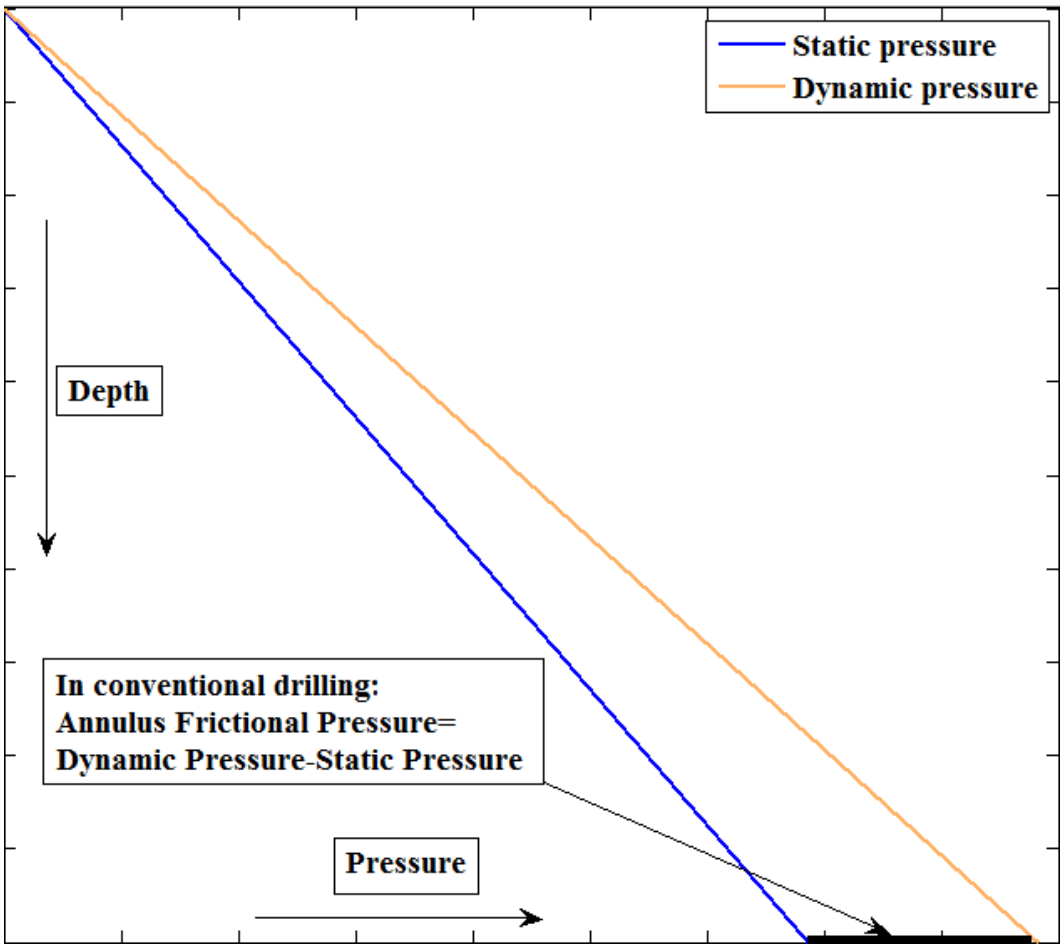

Figure 2: Illustration of downhole pressure with conventional drilling concept (modified after [3])

The mud density is manipulated to obtain the correct downhole pressure with conventional drilling concept. Hydrodynamic pressure fluctuation lead to downhole pressure variations during conventional drilling.

In MPD, it adds a surface backpressure, the technology manage to control and maintain a bottom-hole pressure by tuning surface backpressure whether circulating or not (both dynamically and statically). Backpressure may be applied to prevent well flow when circulation is ceased. In this way, keeping the pressure slightly above the highest pore pressure in the drilling window during operation. In turn, a safe operation condition is established. The following equation is generated:

$P_{downhole} = P_{static} + P_{dyn} + P_{back}$ [24] [25]

2.6 Two approaches of MPD

2.6.1 Proactive MPD

Proactive MPD involves designing the well and planning the drilling program in advance in order to extract the benefits of the ability to actively and precisely control the annular pressure profile throughout the drilling operation. [3]

2.6.2 Reactive MPD

The well is equipment conventionally with at least a rotating control device (RCD), dedicated choke and drillstring non-return valve to enable technology to more safely and efficiently deal with unplanned downhole pressure developments. Reactive MPD uses only MPD technology as a contingency to diminish drilling troubles in case they appear. [3]

2.7 Basic MPD equipment/elements

Fig. 3 shows the schematics of MPD system including the basic elements (rotating control device, rig choke manifold, mud gas separator).

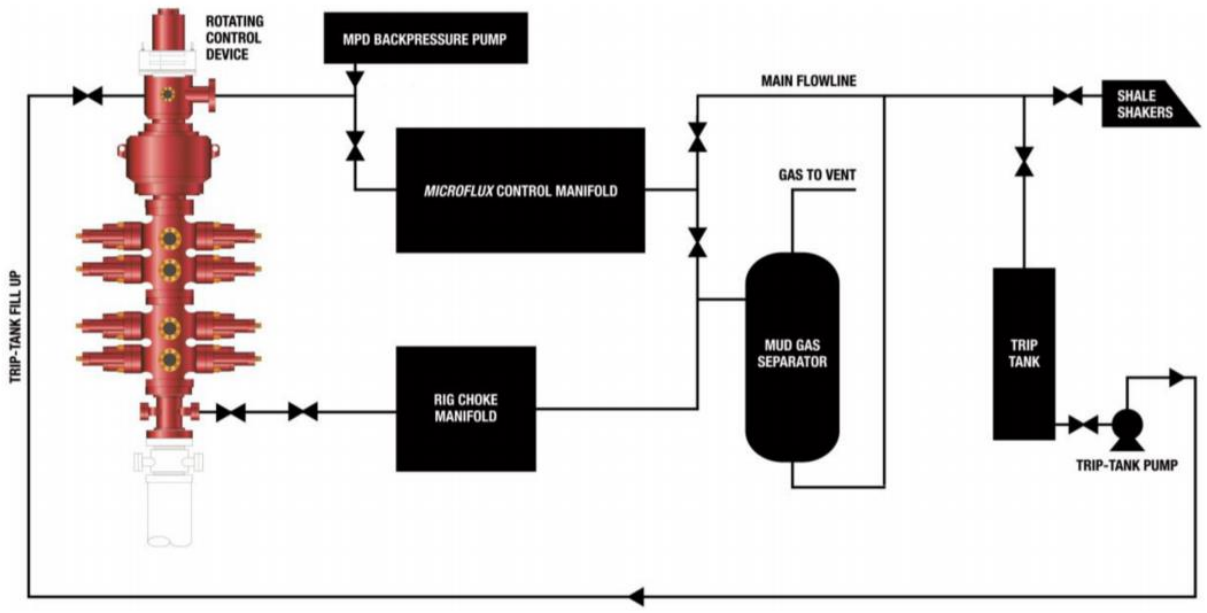

Figure 3: MPD piping and instrumentation diagram [4]

2.7.1 Rotating Control Devices (RCD)

One of the essential pieces of equipment in MPD is a rotating control device. By utilization of RCD, enables the drilling fluid flow to through the MPD choke manifold instead of rig flow line, which is open to the atmosphere.

RCD is usually installed on the top to the rig annular blow out prevent (BOP). During drilling operation, it is utilized for the intention of creating a pressure-tight barrier on the top of annulus while the drillstring rotates. [26]

RCD enables diverting of flow through choke to separation equipment thereby reducing associated dangers to rig personnel. RCD is the most common MPD tool and it is the most important protection against escape of well fluids to the atmosphere during critical drilling operations. Today, three-fourths of U.S. onshore drilling programs practice at the least one section with a closed-loop circulating fluid system equipped by a RCD. [27] [28]

In general, when MPD is required, RCD is accepted as standard equipment. In other words, RCD enables MPD technology. [27] [28]

For example, fig. 4 shows a model of 8068 rotating control device from MISWACO , a Schlumberger company is designed to provide annular pressure seal in large-diameter wells up to 30 in. It improves rig safety by isolating the rig floor from potentially hydrocarbon during drilling operations. [5]

Figure 4: Rotating control device [5]

2.7.2 Drill-pipe non return valves (NRV)

NRV is required in the MPD implementation to control U-tube effect. Its function is to allow fluid to flow through it in the right direction during conditions that one end of drill pipe is exposed at surface, for instance, during a pipe connection or tripping operation. [24]

2.7.3 Coriolis mass flow meter

MPD provides a sealed annulus solution that requires accurate flow reading. A coriolis mass flow meter is equipped to allow monitoring of drilling events such as influxes or downhole losses. It isable to distinguish wellbore ballooning phenomena from kicks during pumps shut-off. [6]

Figure 5: Coriolis mass flow meter [6]

It provides high accuracy and stability real-time measurements of

- Density
- Viscosity
- Mass flow
- Temperature
- Volumetric flow [6]

2.7.4 Choke manifold

Choke manifold is a system of valves and chokes. MI SWACO, a Schlumberger company introduces a type of flat design manifold which is shown in fig. 6.

Figure 6: Choke manifold [7]

In MPD, A choke manifold controls the flow of mud from the well and generate a desired back-pressure. A shortage of choke is that it is unable to control pressure when flow is too low or not presented. Thus a pump is mounted into the system to ensure there is an additional flow passing the choke. This auxiliary backflow pump enables to stimulate the flow through the choke, make possibility of controlling the back-pressure. [24]

A dedicated drilling choke manifold in MPD system is classified as manual choke, Semi-automatic (set-point choke) and fully automatic based on its operation. Manual chokes are operated manually through the communication between the choke operator and the driller. [29]

2.8 MPD application with Constant bottom hole pressure (CBHP) technique and (DGD)

Two variants of MPD technology are presented in this section: constant bottomhole pressure (CBHP) and dual gradient drilling (DGD)

- Constant bottom hole pressure (CBHP)
- Dual gradient drilling (DGD)

2.8.1 Constant bottom hole pressure method

CBHP method means drill with a fluid that maintain a CBHP, whether during circulation or in a static condition. When making a connection, BHP reduction is counteracted by backpressure applied by annular backpressure system to prevent formation influxes to the well bore. During drilling, increase annular friction pressure by means of pumping to prevent reservoir influx. The main goal of CBHP method is to precisely calculate the fluctuation in BHP induced by dynamic effects and timely replace with an equivalent backpressure. [30]

The hydrostatic pressure and down hole temperature increasing with depth. An increase in the hydrostatic and dynamic pressure lead to an increase of the equivalent fluid density, while an increase in the temperature lead to a decrease of the equivalent fluid density. Finally, the reverse effect on density by temperature and pressure may offset. [30]

Density of mud run in at the surface does not characterize the mud density all over the wellbore as the drilling fluid property is affected by fluctuated pressure and changed temperature downhole. [30]

According to M.Arnone and P.Vieira 2009, there are real situations where drilling window was only approximately 50-100 psi. Thus, it is vital to consider every single factor that could affect the drilling fluid's property. Comprehensive information on pressure and temperature change are needed when applying MPD CBHP technology. In other words, an effective and successful application of CBHP MPD requires a precise estimation of equivalent circulating density, static BHP and circulating pressure. In other words, CBHP MPD provides ability of accurately controlling of the annular pressure profile. [30]

2.8.2 Dual gradient drilling (DGD) method

Dual gradient drilling is accomplished via a parasite string or a concentric casing. By inject less-dense fluid such as gas or light liquid at a predetermined depth in the wellbore. The density of the drilling fluid is reduced from that point up to the surface. Purpose of injecting this gas or light fluid is to maintain the bottom hole pressure above the formation pore pressure and prevent gross overbalance thus not fracturing the well. Consequently, a light fluid occurs in the upper part of the injection point and a more dense fluid exists below the injection point. [25]

Fig. 7 shows the pressure profile of the dual gradient drilling method. One lower density gradient above 10000ft and one higher density gradient below 10000ft in a well.

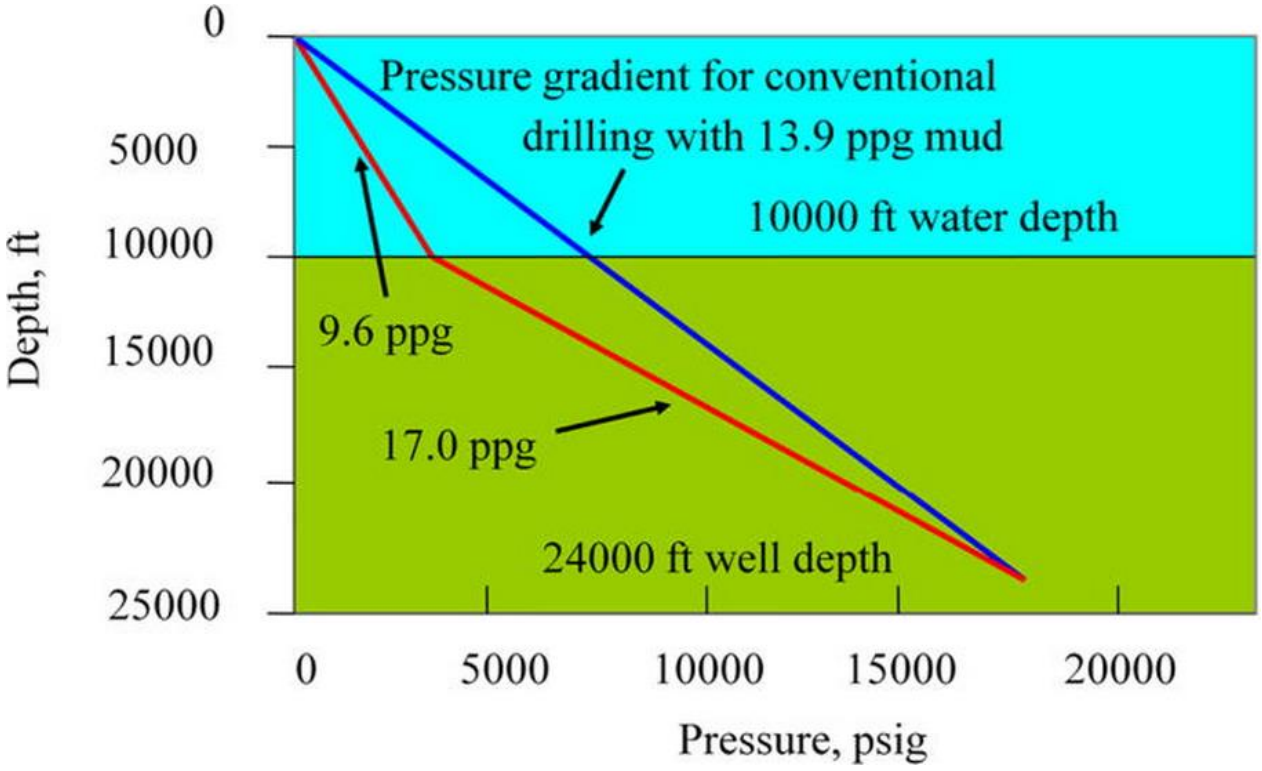

Figure 7: Pressure gradient profile for dual gradient method [8]

2.9 Main benefits of MPD

- Diminish safety risks, provide more precise wellbore pressure control, reduce NPT and improve drilling efficiency,
- MPD provides the operator a wider drilling window, and fewer casing strings are needed to reach the target depth. Thus, the technology permits installing of larger production

casing downhole, thereby minimizing the risk of the production rate from being choked back by small production tubing. It makes larger hole available for oil and gas production,
- MPD ensures better cement jobs due to closed-loop cementing,
- The penetration rate is increased, [27] [31]
- MPD system enables a reduced mud weight compare with conventional drilling, hence decreasing the ECD and results in reduction of losses risk during drilling operations. [32]

In a dynamic situation, when drilling with a pressurized and closed system by ultilizing MPD method, the risk of meeting well control problems are strongly reduced. It helps to detect influxes from reservoir and size of influx is also reduced. In addition,by appling of an automated MPD choke system, more precise control of BHP achieved while circualting out small influxes. [33]

3 Control theory

3.1 Introduction

Control theory is a relatively old subject. It is involved in every engineering discipline, including oil and gas, robotics. Commonly deals with the dynamical behavior of the system. A good control system should provide stability with steady state accuracy. In the following section, those are discussed:

- Concept of control theory
- Feedback control(PID) and feedforward control
- Tuning method (The good gain method from Finn Haugen)

A block diagram of a control system is shown in fig. 8. There are two input signals to the control system, one is termed as *reference* (r) and the other is disturbance. The reference is often named as setpoint. Reference can be a fixed or varying value. In automatic MPD, when driller pumping, the flow rate is defined as one of the manipulated variable in the process. A value of *error* (e) is determined as the difference between reference and the *process output variable* (y). Finally, this simple mathematical relation is obtained $e = r - y$.The value of control error e expected to be small, preferable zero. Less e indicates higher performance of the control system. Controller's functionality is to display the process output variable and compare it with the reference. [34] [35]

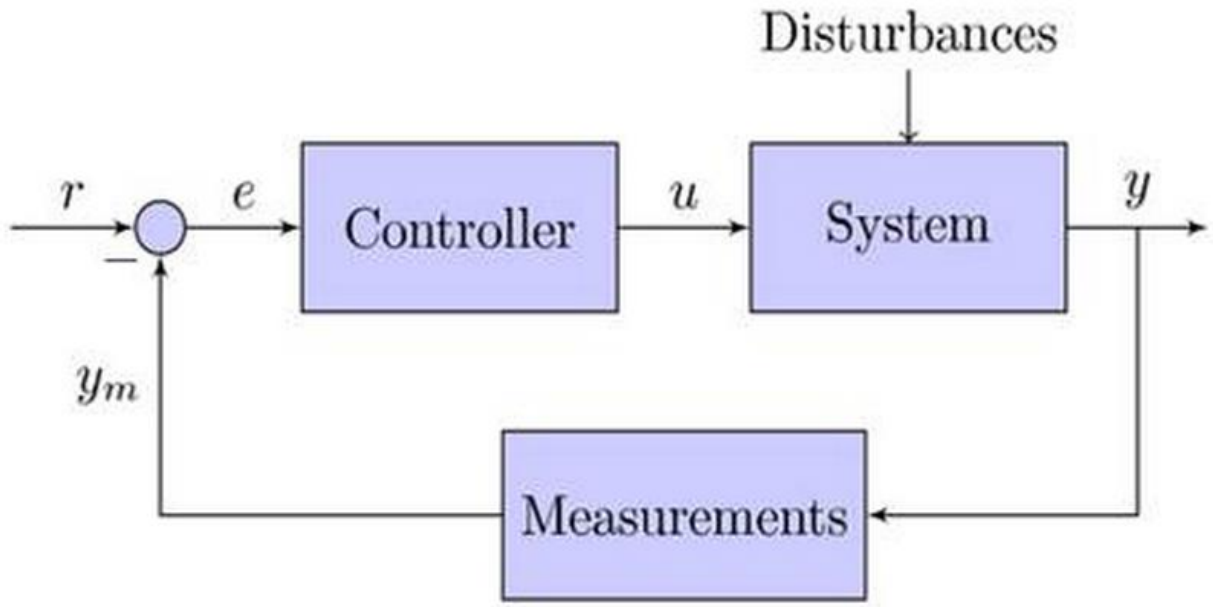

Figure 8: A block diagram of a control system [9]

In the figure: where

u=control value or manipulated variable, can be pump flow rate, choke valve opening in MPD drilling system.

y_m= process measurement.

In the system box is what we want to measure, for example, pressure, temperature.

The disturbance is a non-controlled input variable in the process that affects the process output variable. [11] [35] [34]

3.2 PID controller

PID controllers are widely spread in all areas.

Today, more than 95% (Åstrøm and Murray 2009) of the control loops are of PID form in industry process control. The process control including manipulating variables, controlled variables and process.

A proportional-integral-derivative controller (PID) is a control loop feedback mechanism broadly used in industrial processes because of their simple structure and adequate performance. PID control is the most common form of feedback control. The role of this feedback controller is to

calculate an error value as the difference between a measured process variable and a desired set point (reference). [36]

The PID control scheme is called after three correcting terms, the proportional, the integral and derivative values, denoted P, I, and D respectively. The performance of a PID controller depends on tuning of its parameters. [36]

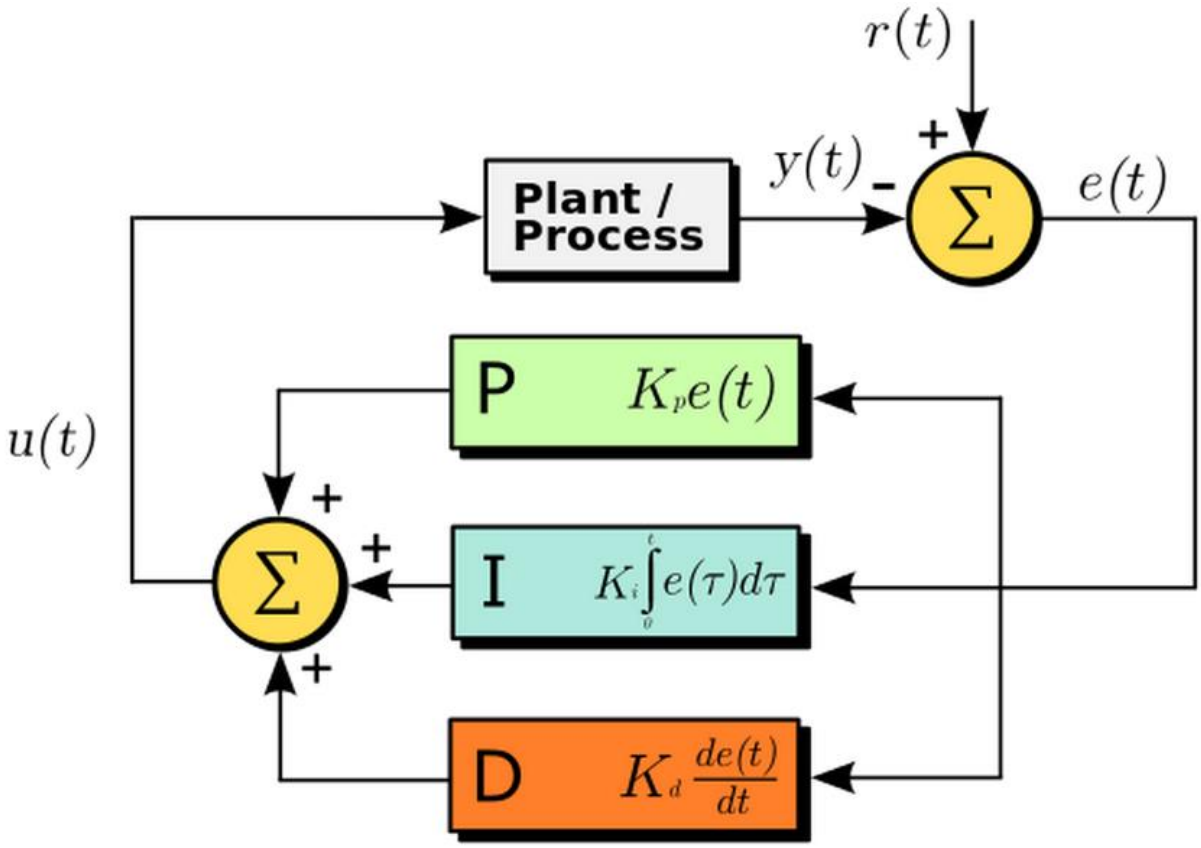

Figure 9: A PID controller [10]

The idea PID control algorithm is written by

$$u = u_0 + \underbrace{K_p * e}_{u_p} + \underbrace{\frac{K_p}{T_i} * \int_0^t e d\tau}_{u_i} + \underbrace{K_p * T_d * \frac{de}{dt}}_{u_d} \quad (3.1)$$

Where

$k_p = proportional\ gain,$

$k_i = integral\ gain,$

$k_d = derivative\ gain,$

$u = controller\ output\ or\ the\ manipulated\ variable\ (MV),$

$u = u_p + u_i + u_d,$

$u_0 = the\ nominal\ value\ of\ the\ control\ valve,$ (The operator *can* adjust it when the controller is in *manual mode*, and it *can* usually *not* be adjusted when the controller is in *automatic mode*),

$e = control\ error,$

$T_i = the\ integral\ time,$

$T_d = the\ derivative\ time,$

Note that, the process output variable is the variable to be controlled so that it becomes closer to the reference.

The goal of control is to make the process output variable y, follow the reference value (also called set-point value) r. This is obtained by tuning the process inputs (control value, or also manipulated variable) u. The PID controller automatically recalculate and re-adjust the actual measurements to the reference values when there is a change in the reference value.

The error e is defined by $e = r - y$. By tuning these three parameters in the PID controller algorithm, the controller manage to solve control problems properly. [34]

Proportional term

$$u_p = K_p * e \qquad (3.2)$$

The proportional term gives an output value, which is proportional to the current error value and reacts suddenly, and this fact makes a high proportional gain creates a larger transformation in the output for a certain change in the error. Conversely, a small gain produces a less sensitive controller.

With a high value of gain causes a strong control action, in contrast, a too small gain makes it impossible to response to the system disturbances.

Integral term

$$u_i = \frac{K_p}{T_i} \int_0^t e d\tau \qquad (3.3)$$

As the integral term shows, it being calculated as the time integral of error e, that means this term presents the total amount of the continually error during a given time period. [34] [10]

Derivative term

$$u_d = K_p * T_d * \frac{de}{dt} \qquad (3.4)$$

Look at $\frac{de}{dt}$, from a pure mathematically view, when error e is positive, $\frac{de}{dt}$ becomes positive thus derivative term produces a positive value to the overall control signal u when K_p and T_d assumed as positive. On the contrary, derivative term contributes a negative value, in other words, it reduces the value of overall control signal u.

In general, positive time derivative $\frac{de}{dt}$ shows faster control and negative value produces a breaking or stabilizing control action. [34] [10]

3.3 Feedforward control

To meet control requirements when reference changes and the process is disturbed, a feedforward control is the remedy used to improve the controller in the system. Feedforward gives direct return from the controller because of adjustments of disturbances or reference. The limitation with implementation of pure feed forward control is that it does not allow adjustment after a control signal has been sent. Correction can only be made via a new control signal. [37]

Feedforward control consists feedforward from disturbance and feedforward from the reference. Typically, in a tank modelling, feedforward term from disturbance has direct effect on valve opening while feedforward term from reference makes the control system respond faster. Feedback term fulfils adjustment of major and minor errors. [11]

3.31 Feedforward control of a tank with valve

A dynamic model of the level in a tank system is explained here.

As given in the figure 10, the tank is w meters wide, l meters long and h_{max} meters high, the area of the tank can be expressed as:

$$A = wl \quad (3.6)$$

The fluid in the tank is h meters high, the volume of the liquid in the tank can be written as:

$$V = Ah \quad (3.7)$$

The flow through the choke valve q_c can be expressed by:

$$q_c = z_c * k_c * \sqrt{\frac{\Delta p}{\rho}} \quad (3.8)$$

Where

$z_c = choke\ valve\ opening,$

$k_c = valve\ constant,$

$\Delta p = p_1 - p_0, the\ pessure\ difference\ across\ the\ valve,$

$\rho = density\ of\ liquid,$

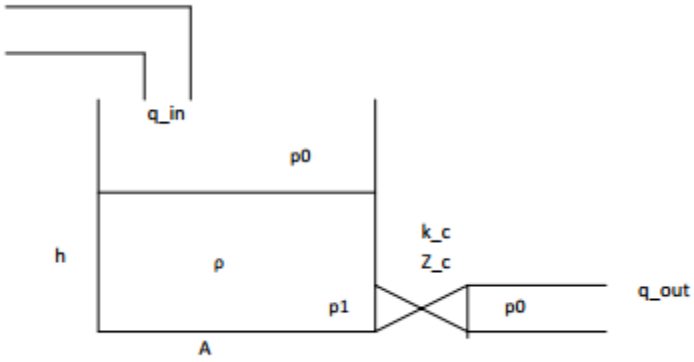

Figure 10 Drilling fluid tank [11]

The figure 10 illustrates the flow rate into the tank system is q_{in}, $q_c = q_{out}$, As the mass balance says: Mass rate in = Mass rate out, then the dynamic liquid volume in the tank can be given as:

$$\frac{dV}{dt} = q_{in} - q_c \quad (3.9)$$

The level dynamics of h in the tank is:

$$\dot{h} = \frac{1}{A}(q_{in} - q_c) \quad (3.10)$$

The pressure p_1 is can be expressed as:

$$p_1 = \rho * g * h + p_0 \quad (3.11)$$

Where

$\rho * g * h = hydrostatic\ pressure,$

$p_0 = atmospheric\ pressure,$

Flow rate out through the choke can then be given by:

$$q_c = z_c k_c \sqrt{gh} \quad (3.12)$$

A dynamic model of the tank (or change in pit level with time) can then be written as:

$$\dot{h} = \frac{1}{A}\left(q_{in} - z_c k_c \sqrt{gh}\right) \quad (3.13)$$

By rearranging the equation, the following equation is obtained:

$$\dot{h}A = \left(q_{in} - z_c k_c \sqrt{gh}\right) \quad (3.14)$$

The choke valve opening can be written as:

$$z_c = \frac{q_{in}}{k_c\sqrt{gh}} - \frac{\dot{h}A}{k_c\sqrt{gh}} \quad (3.15)$$

By assuming $\dot{r} = \dot{h}$, the foundation for designing the feedforward terms for the reference and the disturbance in a tank system can be written:

$$z_{cf} = \frac{q_{in}}{k_c\sqrt{gr}} - \frac{\dot{r}A}{k_c\sqrt{gr}} \quad (3.16)$$

When neglecting changes in the reference ($\dot{r} = 0$), the system with feedforward term from the disturbance is obtained:

$$z_{cf} = \frac{q_{in}}{k_c\sqrt{gr}} \quad (3.17)$$

When neglecting flow rate ($q_{in} = 0$), the system with feedforward term from the reference is obtained:

$$z_{cf} = \frac{\dot{r}A}{k_c\sqrt{gr}} \quad (3.18)$$

[11]

3.4 With only feedback vs feedback plus feedforward

The ideal behind the feedback control is to reduce the control error because of the inevitable imperfect feedforward control. Feedforward control is often based on a mathematical process model, it requires known values through measurements of all variables in the model at all times. Because of this, the flawlessness of feedforward control is limited. [34]

With feedforward control in addition to feedback control results in significantly optimized control performance. [11]

Fig. 11 shows choke pressure when making a drillpipe connection.

The choke pressure with only feed-back control- or error-based control, the measured pressure signal is quite smooth when following ramps after 250 seconds and after 650 seconds. The downside is that measured choke pressure deviated visibly from the reference. Additionally, there is a pressure fluctuation in the measured choke pressure just before ramping up the rig pump.

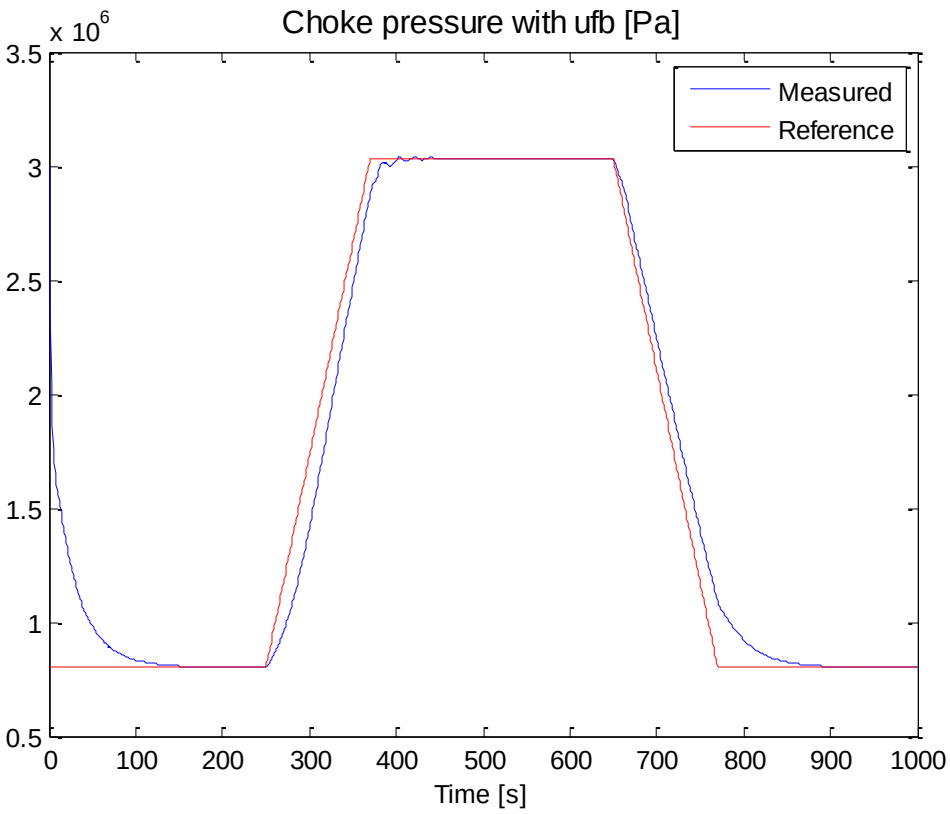

Figure 11: The responses of a feed-back control, (modified after [12])

Fig. 12 illustrates the choke pressure with feed-back control including feed-forward terms of disturbance and reference.

In this case, the error between measured choke pressure and reference reduced meaningfully by including feed forward term. The overall control performance improves significantly.

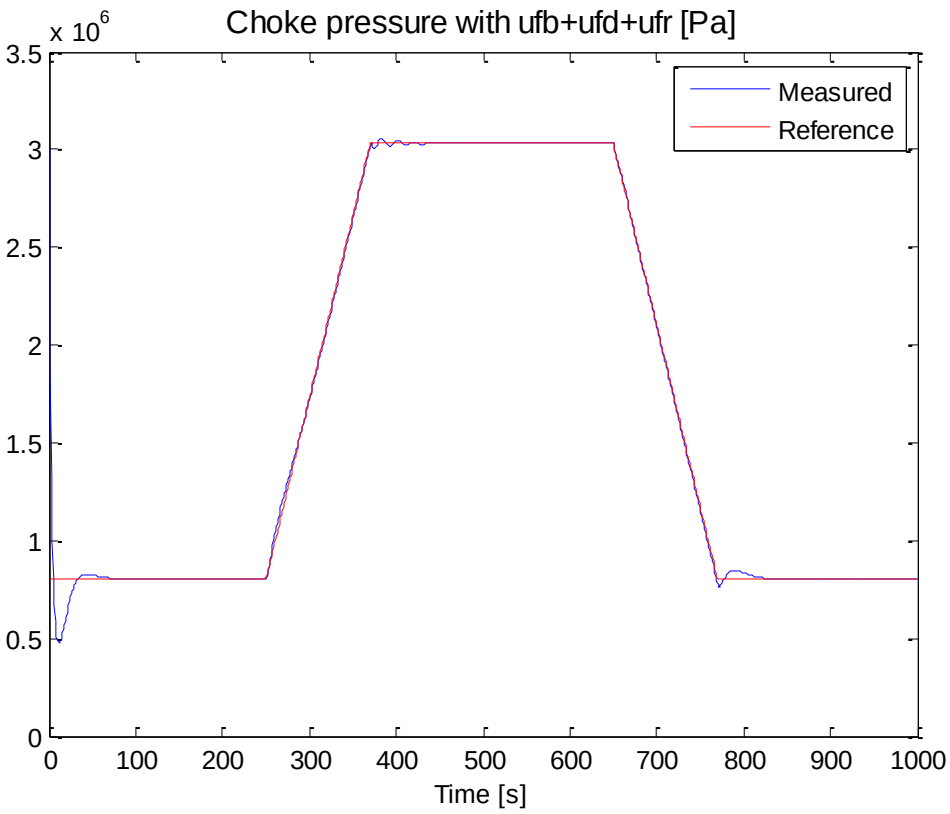

Figure 12: The effect on choke pressure by adding feed-back control including feed-forward terms of reference and disturbances. (modified after [12])

3.5 The Good Gain PID tuning method (Finn Haugen)

Many parameters contribute to an unstable and non-smooth process operation, tuning is one of them.

Feedback control system will be unstable when input of controller parameters are uncertain or erroneous, thus good stability and fast responses are essential topics in the control theory.

A large number of tuning methods have been established for control design can be applied to PID control. The Good Gain method is presented in this part.

- Stage 1: Start with adjust the nominal control signal u_0 in order to bring the process closer to the normal operation point.
- Stage 2: Make sure one is working with a pure P controller by setting $T_i = \infty$ (or to a relatively high value) and $T_d = 0$ (in some commercial controllers T_i is set equal to zero to deactivate the integral term. Alternatively, one begins with $K_p = 1$, then adjust the K_p value until some overshoot are shown and a hardly undershoot displays. (or vice versa when one making a negative step change). The gain value is named as K_{PGG}. It is

important to point out that the control signal shall not operate to any upper limit or lower limit during the tuning. If this is a case, K_p value will be too large or too small to delivery good stability to the control system in a normal operation. Usually, 5% of the reference range is acceptale.

- Stage 3: Set the integral time T_i equal to $T_i = 1.5\ T_{ou}$. Where T_{ou} is defined as the difference between the overshoot and undershoot of the step response with the P controller. When system contains more than one integrator, there will be offset from reference since the controller during the tuning is a pure P controller.
- Stage 4: Stability of controller is decreased when the I-term is added into the system. In order to compensate for this stability reduction, the value of K_p can be reduce to 80% of the initial value. The relationship is expressed as : $K_p = 0.8k_{PGG}$.
- Stage 5: By setting $T_d = \frac{T_i}{4}$ to include the D term into the system.
- Stage 6: Finally, in order to check the stability of the control system with the above controller settings, a step change of the reference is required. By re-adjust the controller gain combined with raise the integral time, the stability of the system will be improved. [34]

4 Modelling

4.1 Introduction

In this chapter the model formulations are presented for later simulating and analyzing of MPD during connection event. The following models are included/considered:

- Density model
- Kaasa model

4.2 Density model

When study dynamic process, based on the laboratory data we need to write equations or mathematic descriptions of the dynamic process. Partial differential equation is one of the solutions.

The general form of density can be written as

$\rho = \rho(p, T)$ (4.1)

Where p is the pressure, ρ is the density and T is the temperature.

Since the changes in density as a function of pressure and temperature in general are tiny for a liquid, a linearized equation is commonly utilized to describe the density:

$$\rho = \rho_0 + \frac{\rho_0}{\beta}(P - P_0) - \rho_0 * \alpha * (T - T_0) \quad (4.2)$$

Where

$$\beta = \rho_0 * \left(\frac{\partial p}{\partial \rho}\right)_T \quad (4.3)$$

$$\alpha = -\frac{1}{\rho_0} * \left(\frac{\partial p}{\partial \rho}\right)_T \quad (4.4)$$

Where ρ_0, p_0, and T_0 are defined as the reference point for the linearization,

$\beta = the\ isothermal\ bulk\ modulus\ of\ the\ liquid,$

$\alpha = the\ cubical\ expansion\ coefficient\ of\ the\ liquid,$

In the case study two, Assuming $T_d = T_a = T$ and $\rho_d = \rho_a = \rho$, it means the operation is demonstrated without considering fluid temperature difference between drillpipe and annulus. Note that the calculated T_d was selected as the final temperature in the simulation. Density linearization equation (4.2) can be rewritten as:

$$\rho_d = \rho_0 + \frac{\rho_0}{\beta_0} * (P - P_0) - \rho_0 * \alpha * (T_d - T_0) \quad (4.5)$$

Where

$T_d = Drillpipe\ temperature,$

$T_a = Annulus\ temperature,$

$\rho_d = Drillpipe\ density,$

$\rho_a = Annulus\ density,$

[11] [38]

For practical reason, assume isobaric condition in the well and the pressure is calculated as the middle-point value. (The average of surface and hydrostatic pressure). The pressure in the well is:
$P = \frac{\rho_0 * g * h + P_{atomospheric}}{2}$

Table 1 Values for calculating of pressure

$\rho_0[kg/m^3]$	$g[m/s^2]$	$depth\ of\ well[m]$	$P_{atomopheric}[Pa]$
1600	9.8	$h_1 = 4800\ in\ case\ one$ $h_2 = 1951\ in\ case\ two$	1.013×10^5

Bulk modulus β relates to the stiffness of the fluid and is reciprocated with the compressibility of the liquid, $c = \frac{1}{\beta}$. Since the bulk modulus describe the dominating pressure transients in the system, it is defined as the most important property in determining the dynamics of the hydraulic system. [13]

Downhole pressures are influenced by density in the tubing. The impact of temperature and pressure on fluid density especially for high temperature and high pressure (HTHP) wells can result in wrongly evaluation of density in the wellbore and incorrectly calculation of the bottom hole pressure. The consequence can be difficult and dangerous as the drilling window is commonly small for HTHP wells. It could be influx into the well or mud loss to the reservoir. [39]

The next figure compare the true densities with predicted densities for temperature ranges from 0 to 200 degrees and pressure ranges from 0 to 500 bar. The following parameters are used to plot the figure 13. The MATLAB codes are in the appendix.

Table 2 Density model variables.

parameter	value	unit
β	1.545×10^4	bar
α	5.4489×10^{-4}	
ρ_0	0.016×10^5	kg/m^3
p_0	9.3202	bar
T_0	20	℃
T	4; 20; 50; 75; 100; 125,150; 175; 200	℃

Fig 13. shows the density and pressure vs temperature for the temperature range from 0-200 degrees and the pressure range from 0-500 degrees. The graph illustrates the drilling fluid density as a function of temperature and pressure. The density model applied to plot this figure is discussed previously.

It is important to point out the resulting error by neglecting dependence on the temperature may be considerable. This is illustrated in fig. 13. In this case, when pressure is 490 bar, at temperature 50 degrees gives a density of $1620\,\frac{kg}{m^3}$, at the same pressure point, at temperature 100 degrees result in a density of $1580\ \frac{kg}{m^3}$, the resulting error in density is sum to 40 $\frac{kg}{m^3}$ when temperature effect is not included . When assuming a well is 2000 meters deep, the resulting error in BHP will be 40 $\frac{kg}{m^3}$ *g*2000meters = 7.8 bar. It can be imagined how significantly the BHP deviation will be in deep-water and HTHP wells if temperature effects have not been counted in density estimation. For HTHP wells, these effects is very important to the successful drilling due to the restricted safe drilling window.

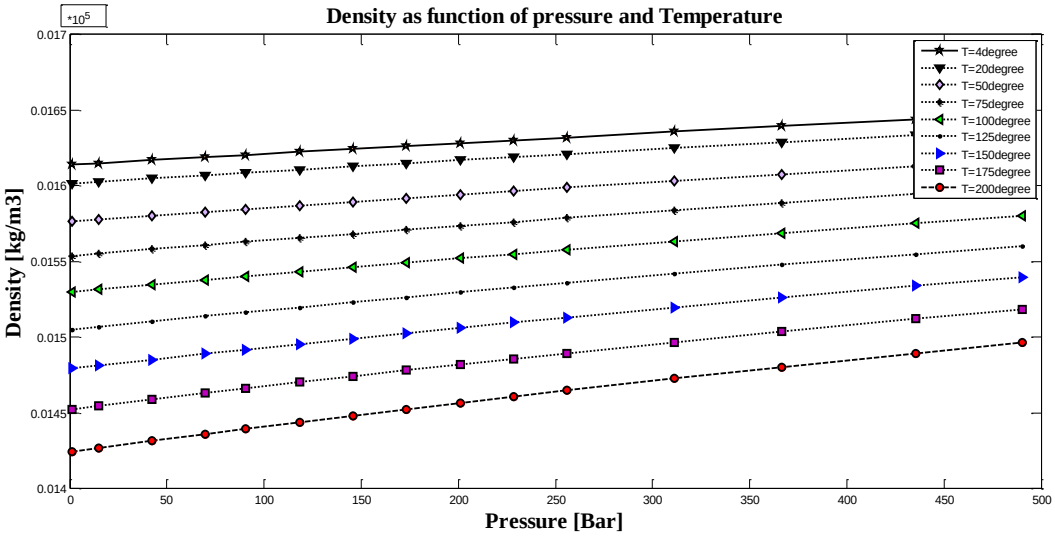

Figure 13: Effect of pressure and temperature on the density of the 1614.06 $\frac{kg}{m^3}$ mud

Data source [40]

The figure 14 illustrates the difference between true densities and measured densities. The data used to plot the figure 14 is in the appendix.

At temperature equals 4, 20, 50,75,100, and 125 degrees, the predictions by using of the density model agree very well with measured density at the pressure range from 0-500 bar. It shows a relatively high accuracy. Plot gives some small deviations at temperature equals 4 degrees,175 degrees and 200 degrees, but it is acceptable. This, again the results are reliable by using the density model in temperature ranges from 0-200 degrees and pressure ranges from 0-500 bar. And it has been verified by (P.Isamourg et al. 1996 [41]) This accuracy condition will be disturbed when the pressure and temperature exceeds their temperature and pressure respective ranges. [38]

The true density curves show that when changing pressure from 0 to 490 bar at 200℃, the density of the drilling fluid increases 90 $\frac{kg}{m^3}$ ($from\ 1410\frac{kg}{m^3} \rightarrow 1500\frac{kg}{m^3}$), while varying temperature from 4℃ to 200℃ at 0 bar results in a density reduction of 190 $\frac{kg}{m^3}$ ($from\ 1610\frac{kg}{m^3} \rightarrow 1420\frac{kg}{m^3}$).

When assuming a vertical well is 1900 meters, if changing pressure from 0 to 490 bar at 200℃, it gives a *pressure increase* of $\left(90\ \frac{kg}{m^3} * g * 1900m = 16.78\right) bar$, while the *pressure decrease* will be $\left(190\frac{kg}{m^3} * g * 1900m = 35.41\right) bar$ if vary temperature from 4℃ to 200℃ at 0 bar.

The result indicates that temperature is more dominant on density for the current type of drilling fluid.

Figure 14 also illustrates that at lower temperature points, the slope of true density profile is lower compare with slope of true density profile at higher temperature points.

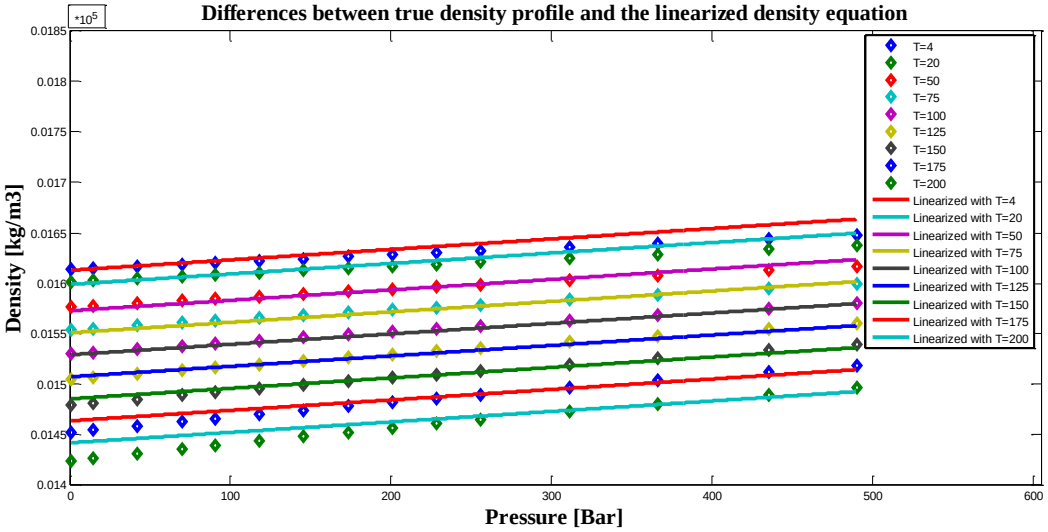

Figure 14: Comparison of true density and linearized density, two different behaviors are caused by temperature and pressure effect of 1614.06 $\frac{kg}{m^3}$ mud

Data source [40]

4.3 The Kaasa simplified wellbore model

Kaasa model is named after Glen-Ole Kaasa. The mathematical development of his model is shown:

Typically, in a simplified dynamic model the dependence on the temperature is eliminated due to the thermal expansion coefficient α for liquids is normally small, thus Eq.(4.2) can be expressed as

$$d\rho = \frac{\rho_0}{\beta} dp \qquad (4.6)[13]$$

The fact is that neglecting the effect of temperature on fluid density especially for high pressure and high temperature (HTHP) wells can cause wrong estimation of density. The heating of drilling fluid causes extremely fluctuations on the BHP in HTHP wells. The incorrect estimation of BHP is produced by expansion or contraction of the drilling fluid in the well. A gain or a loss in the active mud pit will arise due to this volume changing. This phenomenon was defined as mud ballooning which was analyzed by Eirik Kårstad in 1998. [42]

From the mathematically view, the mass balance for a system without a chemical reaction is as follows:

$\dot{m} = m_{in} - m_{out}$ (4.7)

Mass balance in the standard integral form for a homogeneous control volume:

$\frac{d(\rho v)}{dt} = m_{in} - m_{out}$ (4.8)

Where ρ is the density of the fluid in the control volume.

$\frac{\rho dv}{dt} + \frac{v d\rho}{dt} = \rho_{in} * q_{in} - \rho_{out} * q_{out}$ (4.9)

Where $m_{in} = \rho_{in} * q_{in}$ and $m_{out} = \rho_{out} * q_{out}$ are the flow rates of mass in and out of the control volume, respectively. To obtain a more appropriate form, the following equation is given:

$\frac{v d\rho}{dt} = -\frac{\rho dv}{dt} + \rho_{in} * q_{in} - \rho_{out} * q_{out}$ (4.10)

By substitute $d\rho$ in eq. (4.10) and assuming $\rho_0 = \rho_{in} = \rho_{out}$, let $\frac{\rho dv}{dt} = 0$ since the volume of the drillstring is constant during drilling, the equation can rewrite as:

$\frac{v}{\beta} * \frac{dp}{dt} * \rho = \rho_{in} * q_{in} - \rho_{out} * q_{out}$ or

$\frac{v}{\beta} * \dot{p} = q_{in} - q_{out}$ (4.11)

Where q_{in} and q_{out} defined as volumetric flow rates, with inlet density ρ_{in} and outlet density ρ_{out}.

Consider *two* control volumes; *the first* is when the flow in the drillstring from mud pumps to the bit, q_{in}, will be equal with the mud pump pressure q_p while q_{out} is same as the flowrate through the bit,q_b, the time derivative of the pump pressure can be written as :

$\frac{dp_p}{dt} = \frac{\beta_d}{v_d}(q_p - q_b)$ or

$\dot{p_p} = \frac{\beta_d}{v_d}(q_p - q_b)$ (4.12)

The second is when the flow in the annulus from the bit and up the well through the choke, consider there might be influx from the reservoir, the time derivative of the choke pressure can be described as:

$\frac{v_a}{\beta_a} \frac{dp_c}{dt} = -\frac{dv_a}{dt} + q_b + q_{bpp} - q_c$ (4.13)

Equation 4.13 is then transformed to:

$\dot{p_c} = \frac{\beta_a}{v_a}(q_b + q_{bpp} + q_{res} - q_c)$ (4.14)

Where

$v_a = volume\ of\ the\ annulus,$

$\beta_a = the\ effective\ bulk\ modulus,$

$q_b = the\ flow\ through\ the\ bit,$

$q_{bpp} = the\ flow\ from\ the\ backpressure\ pump,$

$q_{res} = potential\ influx\ from\ the\ reservoir\ to\ wellbore,$

$q_c = the\ flow\ through\ the\ choke.$

In equation 4.13, the flow rate through choke is time-derivative. Since the v_a is time-derivate, this model consider the annulus volume change as well.

The time-derivate of drill bit flow rate expression that established in the Kaasa model is:

$$\dot{q_b} = \frac{1}{M}\left((p_p - p_c) - (F_d + F_b + F_a) * {q_b}^2 + (\rho_d - \rho_a) * gh\right) \quad (4.15)$$

Where

$M = the\ integrated\ density\ per\ cross\ section\ over\ the\ flow\ path,$

$F_d = friction\ pressure\ drop\ in\ drillpipe,$

$F_b = friction\ pressure\ drop\ in\ drill\ bit,$

$F_a = friction\ pressure\ drop\ in\ annulus,$

$\rho_d = density\ drillpipe,$

$\rho_a = density\ annulus.$

Consider the tank modelling in a simplified model of managed pressure drilling system, the flow through the choke valve modelled by Glenn-Ole Kaasa can be given by

$$q_c = z_c * k_c * \sqrt{\frac{p_c}{\rho_a}} \quad (4.16)$$

Where

$k_c = valve\ constant,$

$z_c = choke\ valve\ opening.$

The following equations summarize the Kaasa's dynamic wellbore model:

$$\dot{p_p} = \frac{\beta_d}{v_d}(q_p - q_b) \quad (4.12)$$

$$q_c = z_c * k_c * \sqrt{\frac{p_c}{\rho_a}} \quad (4.16)$$

$$\dot{p_c} = \frac{\beta_a}{v_a}(q_b + q_{bpp} + q_{res} - q_c) \quad (4.14)$$

$$\dot{q_b} = \frac{1}{M}\left((p_p - p_c) - (F_d + F_b + F_a)q_b{}^2 + (\rho_d - \rho_a)gh\right) \quad (4.15)$$

[11] [13] [38]

When consider deep-water and HTHP wells, during starting up of circulation (after drillpipe connection; after the well ceased for a while) significant temperature elevation can occur, the Kaasa simplified wellbore model in MPD operation can be expanded to consider this dominating part of temperature transients by means of adding the full linearized equation of state. However, this is still an ongoing research. [13]

5 Automatic MPD

5.1 Introduction

Drilling using conventional concept becomes impossible in many cases as the complexity greatly increased in today's well.

Operations on a rig are accomplished in mainly four different levels, they are manual operated, mechanized, and remote controlled and automated, or may be combination of them. In automated operation there is no human control on the drilling operation while in remote operated process the whole process is operated by using a remotely operated device. However, to be fully automated is difficult to achieve on a rig today. [43] The following automated MPD methods are touched in this chapter:

- Backpressure pump technique
- Rig-pump diverter (RPD) technique
- Benefits of applying RPD MPD

As the oil industry is not quite optimistic nowadays, oil price goes down. It gives the room for automation development in drilling.

5.2 Why automation?

The level of automation in the oil industry is relatively low today and expected to increase due to:

1. Strict requirement on health, safety and environment (HSE). Automation permits little pressure variation during continuous production and start up, and ceasing of circulation of fluid, in return enhanced safety.
2. Economic issue. Automation minimizes non-productive time (NPT) offering continuously optimization of production.
3. Effectiveness. [44]

The main target of automated MPD are reduce cost and enhanced efficiency in a narrow drilling window environment and maintain steady pressure profile. In order to achieve the target, automated MPD system is applied differently at unlike degree of control, each with unique capabilities, some control backpressure, some ensure continuously circulation, and others realize mud gradient. Variables, for instance pressure, temperature and flow are controlled automatically by means of two operators administering all control loops in a plant from a control room. During the planning phase, depending on factors such as drill states, rig type and complexity of reservoir, the level of automation is determined for that specific application. [45]

5.3 Hydraulic model

Automatic performance of choke manifold including two elements

- A control system with a hydraulic flow model, which calculate the downhole pressure and produce a desired choke pressure on the basis of a preferred downhole pressure reference.
- A feedback control algorithm that actuates the choke manifold to keep the choke pressure in an acceptable range. [13]

Hydraulic model is the most important decision system in the automatic MPD. The physical appearances in a well are expressed by mathematical model. The model makes the automation possible and it determines in which degree the automatic system can achieve. [46]

The accuracy of the model is upgraded by automatic updating of states and parameters via real-time measurements of topside and at the drill bit. [18]

Typically, in a hydraulic model, the following parameters are calculated:

- The surface back pressure the MPD choke need to apply for maintaining a constant BHP
- Downhole pressure
- ECD
- Temperature
- Standpipe pressure [47]

The fig. 15 shows how the hydraulic model, pressure controller and back-pressure pump add into a MPD system to improve automation.

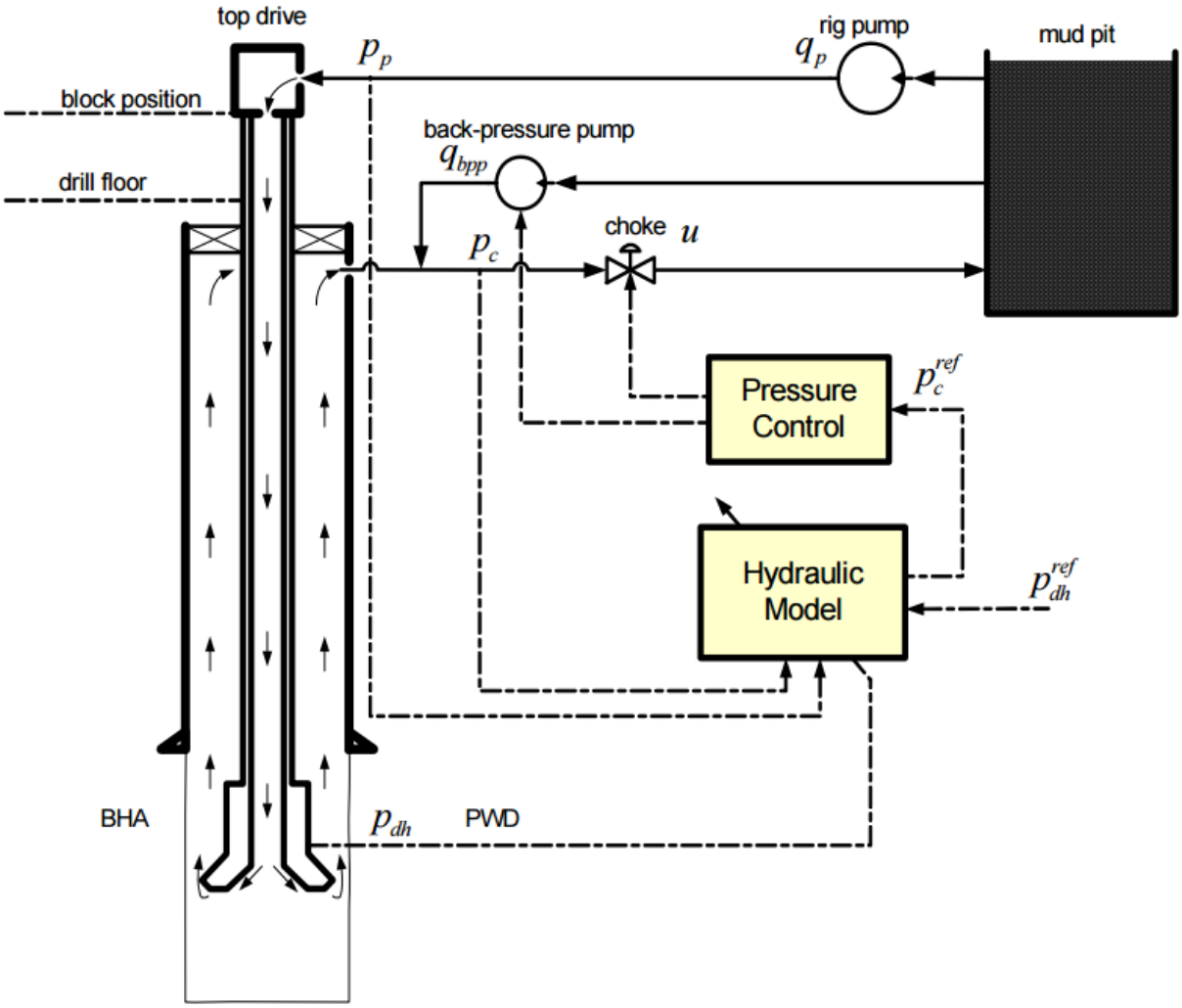

Figure 15: Simplified schematic of an automated MPD system [13]

As it shows in the fig. 15, there are two yellow boxes in the system, a pressure control box and a hydraulic model box. The downhole pressure P_{dh} is measured at all times. The hydraulic model box consists a downhole pressure reference P_{dh}^{ref}, it monitors the downhole pressure at all times, when measured downhole pressure P_{dh} is higher or lower than the downhole reference pressure P_{dh}^{ref}, the hydraulic model gives the message to the pressure control, moreover the signal is sent from the pressure control box to the choke and makes it automatically close or open. [13]

5.4 General overview of backpressure MPD

The BHP comprises of three components, which discussed in the previous MPD theory section:

Hydrostatic head of mud column; frictional pressure which is a function of flow velocity, hole geometry, fluid properties or surface roughness; and surface back pressure. Sudden movements such as when making connection or trips make it hard to keep a stable BHP. [14] [48]

Backpressure MPD can be executed either by manual operation of the MPD choke or automatic controlled choke which requires use of control algorithm.

In manual MPD system, close the choke is done by communication and teamwork between the driller on the drill chair and the choke operator in another room. typically, a table is available, it shows how much backpressure is needed for different flow rates, the choke position is adjusted accordingly with the applied backpressure. How fast the choke can respond is only depending on the choke operator's skill, namely a degree of proficiency. However, no matter how fast a choke operator can respond, it is doubtful that he will ever be fast enough to reply to the loss of pressure caused by an abrupt pump shut-in or other unexpected failures. [18]

Unlike manaual MPD, in automated MPD, the choke movement is done by the control system,when continous stable pressure source is avaible,the autochoke manage to maintain a stable BHP through timely operate the applied surface presure. The system enables the autochoke to perform the same movements at all times. [18] [14]

There is a large misunderstanding and misconception that consistent level of accuracy in all drilling phases can be achieved by a manual MPD system. In reality, in most cases, the accurate and dynamic BHP control is limited only to the on bottom drilling phase. [14]

It is important to note that in order to make the choke in functionality, continuous flow through the choke is required. This pressure source comes from main rig pump during drilling and it is adjust by choke to apply the desired surface pressure. However. when making a drill pipe connection, manual MPD becomes more difficult and complicated. Unfortunately, no flow through the choke means loss of backpressure, furthermore, loss of BHP control. In other words, the consistency of accurate control can be disturbed in some of the drilling phases. Under no flow condition, to increase the surface pressure in order to compensate the loss of dynamic pressure can only be realized if the control system has capability of providing pressure trapping techniques. [18] [14]

An optional remedy was developed. An additional backpressure pump is attached to a conventional MPD system. This supplementary pump provide a continuous pressure source on the annulus when the flow rate from the main pump is not available. Additionally, back pressure pump has usage of cooling the BOP stack by means of circulating cool fluid through the BOP. [33]

With an automated MPD system, increased surface pressure can be achieved by first calculating dynamic friction pressure, and then the control system automatically scales the position sensors to ensure correct measurement. By defining loss of dynamic pressure, the control system is capable of keeping the choke at position at all times, so reduces the necessity of adjusting the choke valve position. In this way, the human failures in repetitive movements is greatly

decreased. Consequently, more stability and more rapidly response time. Thereby increases the consistency of control and efficiency is improved. [49]

Surface choke adjustments and surface back pressure for controlling of the BHP during MPD operation requires accurate downhole temperature meassurement along the wellbore. [19]

It is a step change from manual MPD to automatic MPD. In an automatic MPD system, the control system including downhole pressure estimator and choke pressure controller which can automatically manipulate the choke valve. [14]

BPP method aims to apply surface pressure in typical situations such as when making a drillpipe connection and trips, the main pumps are turned off or ramped down. The BPP is turned on or ramped up to trap this dynamic pressure loss to maintain the BHP at an acceptable range. An improved control level is achieved. [14] [49]

When using BPP the system traps the frictional pressure loss caused by ramping down of rig pump and ramping up of backpressure pump which are shown in the case study 2. The downsides are some pressure fluctuations created at the moments when one pump ramps down and the other ramps up. In drilling of deep water and HTHP wells, the window between pore pressure and formation fracture pressure is narrow, the pressure fluctuations generated through ramping processes are not always accepted since it drives the BHP out of the acceptable range in some cases. A potential well control problem can occur if BHP is not controlled properly in MPD operations. [14]

5.5 MPD using RPD technology

A new method called rig-pump diverter (RPD) was introduced on the base of the foregoing background.

5.5.1 Automation and Control in RPD method

The MPD control system typically adjusts the choke in order to maintain a target BHP. Usually, the BHP can be measured directly with a Measurement While Drilling (MWD) tool, then measurements are received at surface via mud pulse telemetry or telemetry pipe technology. [50]

Typically, the acquisition system has responsibility for gathering, operating and recording data, which has responsibility to maintain the surface backpressure in order to control the BHP at reference level. In this PRD design, Sensors, communications and control interface are three requirements of the automated control system.

- Sensors: In order to provide corresponding physical measurements such as pressure and temperature which are essential for automatically assist connection/diversion process, sensor module including two pressure transducers, one for stand pipe pressure and the

other for diverter line pressure; one flowmeter detect diverter line flow rate; at last, valve and choke position switches.

- Communications: The main communication center consists a dedicated remote input and output (I/O) box, it used for transferring of real-time data (e.g. BHP measurement), status and control data between the RPD and the master programmable-logic controller (PLC) on the automatic choke skid.
- Control interface: The last component of automated control in PRD method is control interface. It comprises a pneumatic control box. By converting electric signals to a pneumatic pulse, valves and chokes are correctly operated in the system. [32] [14]

5.5.2 RPD process

RPD is tailor made for making connection in MPD system.

Rig pump divert (RPD)

The RPD manifold consists:

- An onboard choke
- Valves
- Sensors
- Pneumatic-control panel
- Remote data-input/-output (I/O) devices

[14]

Air, power and a process field bus connection are needed to operate the RPD manifold. Process field bus is a standard for fieldbus communication in automation technology. [51] The main PLC on the MPD choke manifold sends commands to the remote I/O and returns the output values from both the indicators and transmitters on the RPD via the process field bus connection. [14]

RPD step-by-step actions

- First, the stand pipe is required to be fully bled off. First- make sure that there are no returns to the pit from the bleed-off line on the RPD.
- Secondly, it is time to interrupt the connection and add a new drillpipe length.
- At last, once the standpipe valve is closed, the RPD begins directing new fluid from the pumps to the MPD system. According to the desired pressure from the hydraulic fluid model, MPD system utilize the new fluid to carry on maintaining the desired BHP in the well. During the whole operation, control system monitoring the flow split contrasting among the turbine flow meter on the RPD equipment, coriolis flow meter that is mounted on the MPD equipment and the rig pump flow rate.
- In order to confirm the system is fulfilling its flow diverting mission, all three readings must indicate the same values. Once the connection operation is made, driller prepares to drill standard operation again. Meanwhile, the MPD crew keeps on redirecting new flow

back to the standpipe for the purpose of making the condition practicable for the driller to restart the drilling operations. [14]

5.6 BPP vs RPD

The fig. 16 is shown different dimensions of BPP and RPD. The higher one is BPP stand. The size of RPD is dramatically reduced compare to BPP.

In order to make it easy to maintain, all the valves used as diversion equipment are pneumatically actuated which allows to open and close at any speed. With this relatively small size of RPD, it enables to plumb into the MPD system on the ground or on the rig floor. [14]

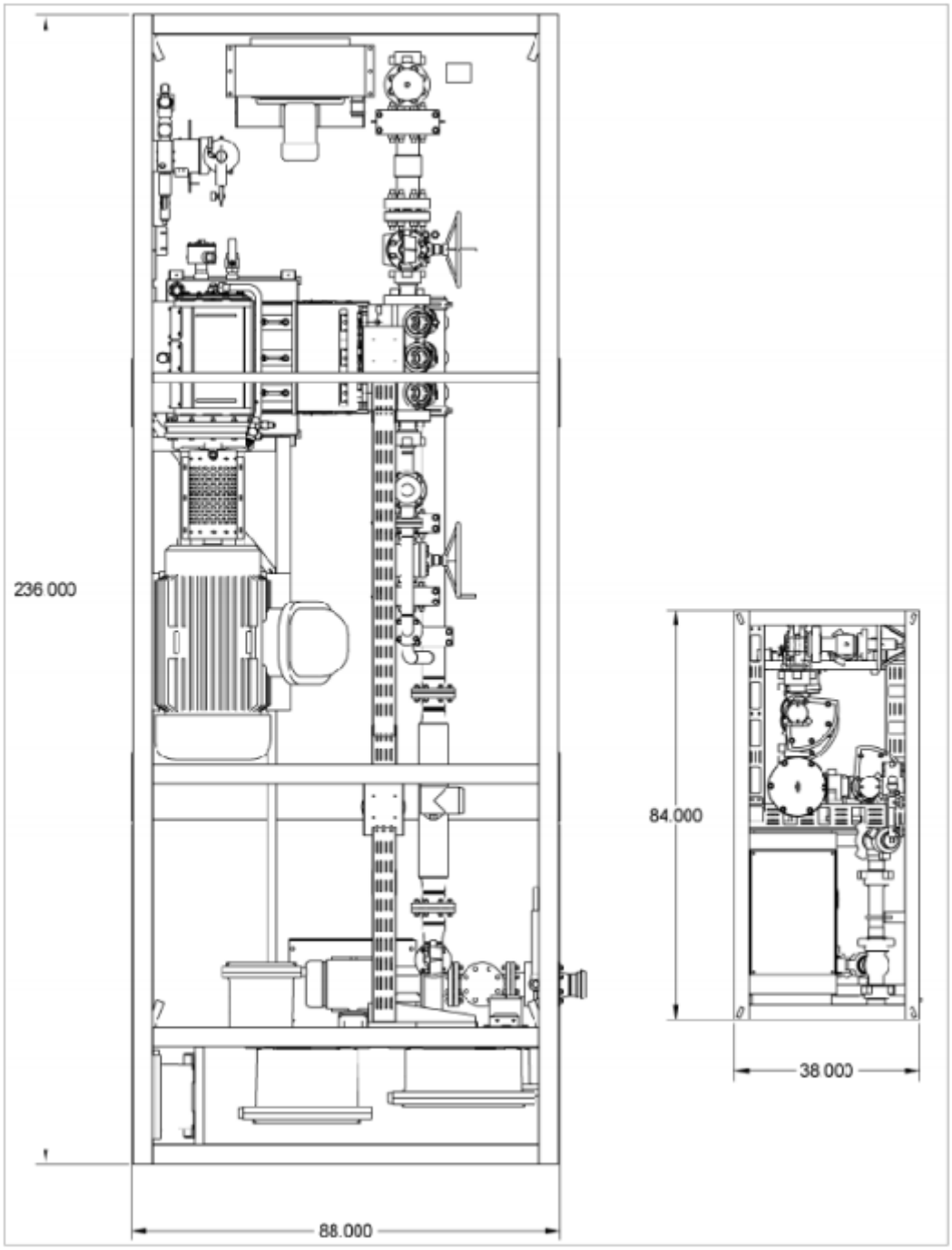

Figure 16: BPP vs. RPD footprint comparisons [14]

Nutshell, making connection with RPD method means directing flow from the standpipe side to the wellbore without using of an additional pump system.

As discussed earlier, during pipe connection, the main concern with the BPP in MPD is ramping up and down of the rig pump. The ramping processes cause oscillation of the MPD chokes. [14]

The design of diverting rig pump eliminates the necessity to shut down rig pumps, yet the automated choke is able to precisely control the BHP constant during drillpipe connection. This enables system to make a smooth connection without pressure spikes. A better control level is realized and a significant improvement for safety is achieved by this technique. [14]

5.7 Benefits of RPD MPD

- The method provides continuous drilling at balance at all drilling phases; eliminate pressure fluctuation during pumps shut-in, realizing a smooth connection, improved accuracy.
- Protect the fracture permeability and formation as it controls the BHP constant.
- Minimizing nonproductive time by limiting unwanted well control problems such as kicks, fluids loss, improved performance. [14]
- People on the rig floor are reduced since the method enables remote operations. [45]
- Larger pressure fluctuations during connection is no longer a critical issue. [14]

6 Temperature model

6.1 Introduction

Drilling in a narrow pore and fracture-pressure window is challenging. If the bottom hole pressure (BHP) is not proper maintained, disaster can occur. Temperature is one of the main issue that result in unstable BHP during operations, especially in HTHP environment where errors resulting from ignoring variations in temperatures can lead to wrongly density evaluation since compressible drilling fluid is usually used in such wells, and compressible mud expand with temperature and compress under pressure, thereby wrongly calculated BHP. [39]

6.2 Circulation process

Predicting downhole temperature changes is an essential part of the well design process. There are two particular solutions for determining temperature profile during circulation:

- Analytical and
- Numerical

Eirik Kårstad has developed an analytical solution to estimate downhole temperature profile in the drillstring and annulus is applied in this study. Several contributions on his subject of downhole temperature predicting have been discussed here.

The starting point for the temperature model is to solve the following two fundamental equations simultaneously to yield both pressure and temperature distributions.

- *The total-energy equation*
- *The mechanical-energy equation* [1]

The circulation of fluid during drilling and completion of a well may be defined as a counter-current heat exchanger with a moving outer boundary as it shown in figure 17. [1]

The process of circulation in a well is usually divided into 3 phases:

- First, fluid comes into the drillpipe;
- Second, fluid passes the drill bit at the bottom of the hole, enters the annulus;
- Finally, fluid flows up the annulus, and arrives at the surface in the end of the trip. [52]

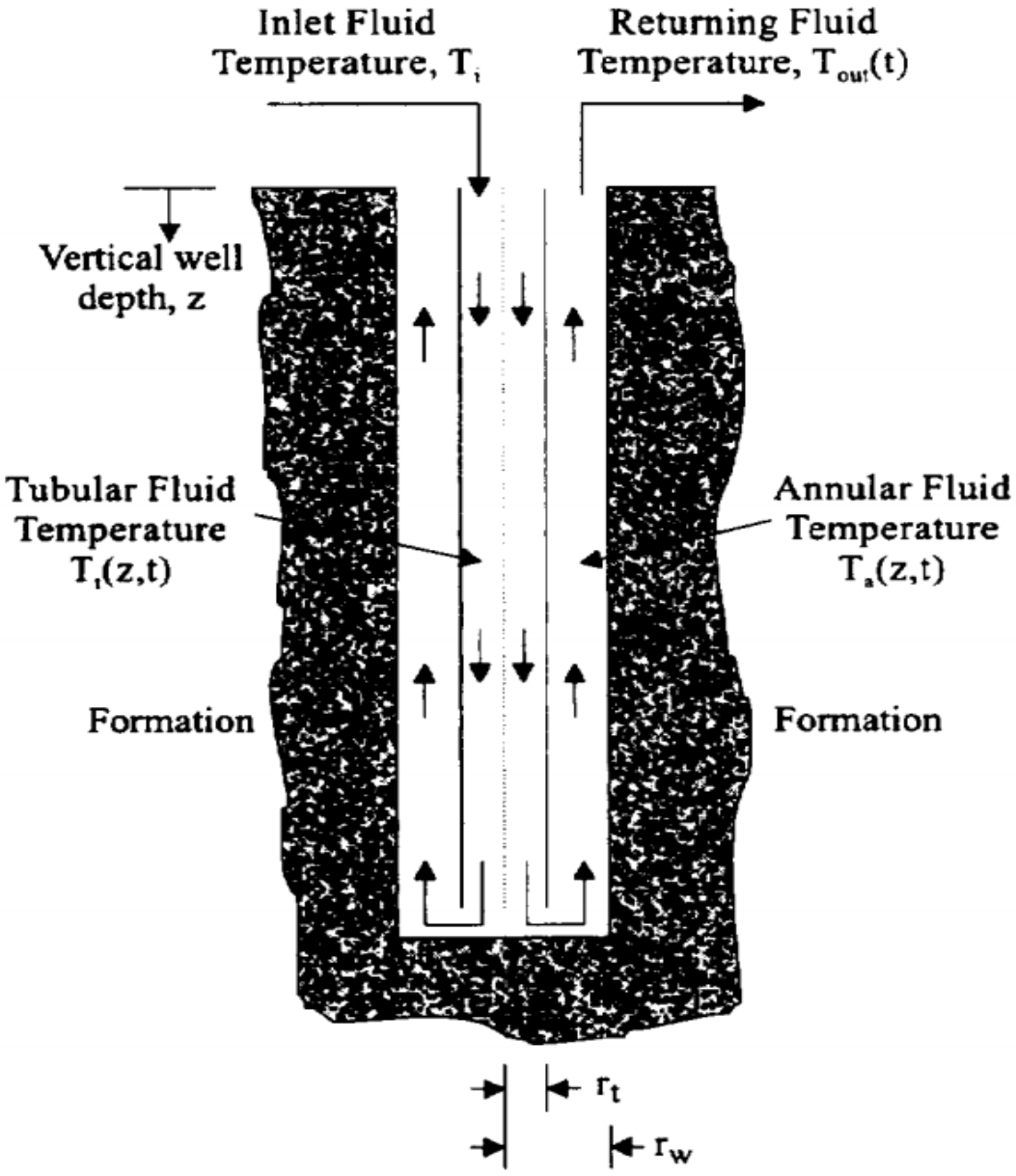

Figure 17: Schematic view of circulating fluid system [15]

However, the following basic assumptions are applied in the model:

- We assume geothermal gradient is constant.
- Transient heat occurs in the formation surrounding the borehole.
- We neglect viscous flow energy, rotational energy, and drill bit energy.

- We assume circulating fluid is incompressible and with a constant circulation rate.

- Neglect axial conduction of heat in the circulating fluid and consider only axial convection.

- We assume the formation is radially symmetric, and the formation is boundless with respect to heat flow.

- We assume the physical properties of the circulating fluid and formation such as density, heat-transfer coefficient, thermal conductivity and heat capacity are constant with temperature.

- Radial temperature gradients in the drillpipe, casing and or annulus are negligible, i.e. the borehole mud is accounted to be mixed thoroughly and can be handled as a perfect conductor during circulation.

- Assume steady-state heat transfer in the wellbore (i.e. independent of time in the well); the heat flow in the tubing and annulus are speedy compared to the heat flow in the formation.
  [1]

6.3 Why predict downhole temperature?

The following reasons have been pointed out why the downhole temperature study is interesting and beneficial:

1. Useful for correlation between wells.

2. Determinate of equivalent static density (ESD).

3. Determinate of equivalent circulating density (ECD).

4. For analyze the pressure/volume/temperature (PVT) modeling of hydrocarbon by using of undisturbed earth temperature profile.

5. Wellhead, production equipment and drill bit design as well as predicting of lost circulation pressure rely on /require knowledge of precise downhole temperature. [1] [53] [54]

6. The temperature variation along the wellbore strengthen or weaken the pressure needed to initiate a hydraulic fracture, in some extent, this gives a solution to control the location of the hydraulic fractures includes in an open wellbore.

7. The thermal-induced stress changes may affect wellbore stability. Temperature cooling disturbs the stress conditions around the wellbore and stress changes induce pore pressure changes, pore pressure decreases with reduced fluid temperature.

8. Predicting of fluid temperature is necessitate to determine the fluid density and viscosity, and conversely to calculate the pressure drop or maximum tolerable pumping rate for varies of operations. [1] [16]

9. For designing of slurry and contribute a successful cement operation. [55]

6.4 Why is there temperature difference between annulus and drillpipe?

First, the cold mud flowing down inside the drillpipe is heated by contact with the pipe wall. It is known that the geothermal gradient increases with depth and hence the return fluids in the annulus, which is in contact with the formation is also exposed to higher temperature with increased depth. This return fluid in the annulus simultaneously absorbs the heat from the preheated drillpipe wall. Consequently, the mud temperature outside of the pipe wall stays higher than the mud temperature inside of the pipe wall since it is being heated by both heat sources.

The following figure shows the downhole temperature profile in drillpipe and annulus in a 2000 meter deep well.

Well and mud data used to simulate the downhole temperature profile are taken from Holmes and Swifte and Kabir et al. The depth is modified.

Table 3 Well and mud data

$well\ data$	$value$	$description$	$unit$
D_o	6 5/8	$Drillstem\ out\ diameter$	in
D_b	8 3/8	$Drill-bit\ size$	in
$depth$	2000	$Well\ depth$	m
ρ_m	1198.264	$Mud\ density$	kg/m^3
q	0.013249	$Flow\ rate$	m^3/s
w	$\rho_f * q$	$Mass\ flow\ rate$	kg/s
ρ_f	2643	$Formation\ density$	kg/m^3
T_{in}	23.889	$Inlet\ mud\ temperature$	℃
T_{sf}	15.278	$Surface\ temperature$	℃
C_{fl}	1676	$Mud\ specific\ heat$	$J/(kg\ ℃)$
K_{fl}	1.73	$Mud\ thermal\ conductivity$	$W/(m\ ℃)$
K_f	2.25	$Formation\ thermal\ conductivity$	$W/(m\ ℃)$
cf	838	$Formation\ specific\ heat$	$J/(kg\ ℃)$
gG	0.023148	$Geothemal\ gradient$	$℃/m$
t	0.02	$Circulation\ time$	hr
U_a	200	$Overall\ heat - transfer\ coefficient\ related\ to\ annulus$	
U_d	100	$Overall\ heat - transfer\ coefficient\ related\ to\ drillstring$	

Data source [16] [17]

Assume homogeneous formation, when drilling a well into the surface, a constant rise in temperature with depth is usually expressed in terms of a temperature gradient. This geothermal gradient characterize as undisturbed temperature before the well is drilled and it is important to be calculated both as a reference temperature and for experiments analysis related to hydrocarbon pressure/volume/temperature performance. [1]

Fig. 18 shows temperature as function of depth shortly after circulation starts. Choosing the surface as reference depth. Hence the downward direction have negative values. The overall effect of circulation heats the formation between the surface and 1075 meters, then to cool the formation from 1075 to 2000meters. The turning point temperature is 40.16 degrees as shown in the figure.

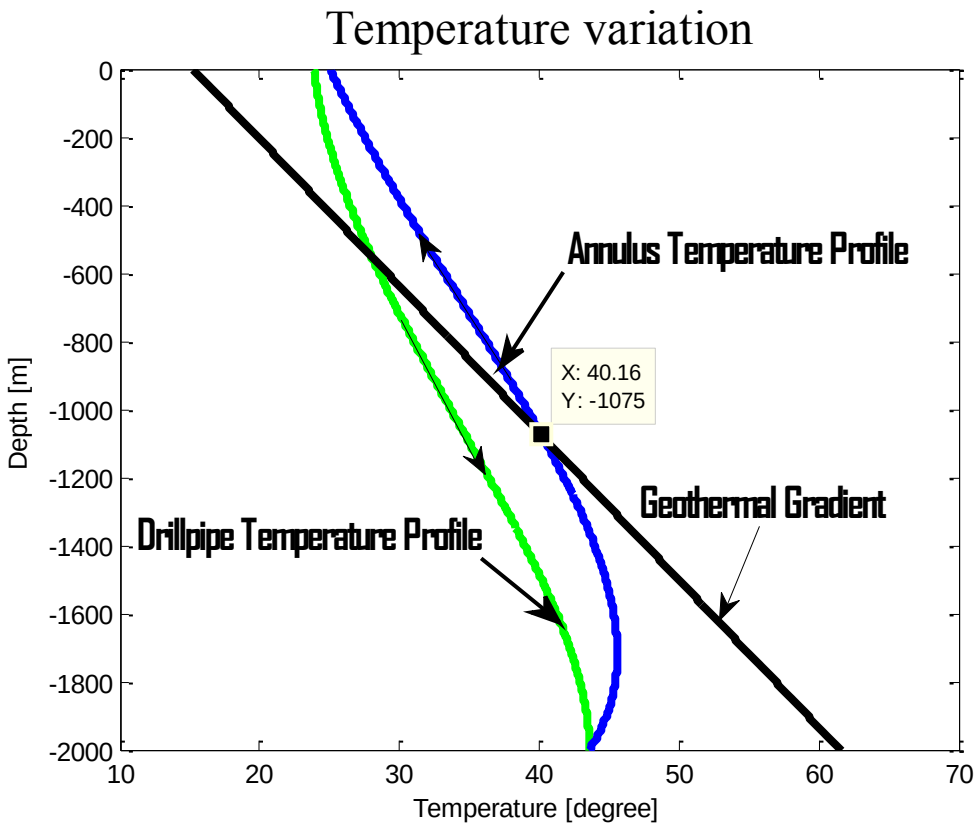

Figure 18: Downhole temperature profile

6.4.1 Maximum fluid temperature

As it shown in the figure maximum fluid temperature does not appear at the deepest point of the well.

The profile of the mud in the pipe/ tubing and mud in the annulus show that the maximum mud temperature occurs in the annular at some depth above the bottomhole. The reason for this phenomenon is temperature of drilling fluid increases gradually as it running down the drill string, temperature is highest at the drill bit, when the fluid begins to flow up the annulus, the surrounding formation transfer heat to it. This gaining in heat overcome the heat loss to the fluid in the drill string. The annular fluid temperature keep on raising until it reaches some depth above the bottomhole that the amount of obtained heat is balanced with the amount of heat depletion. Thus, a peak value of the fluid temperature is measured. [1]

The temperature profile in annular is almost the same as geothermal gradient profile if a well is left under a static condition for a while. When mud pump is restarted, the dynamic process begins and heat exchange between drilling fluid is established again. [56]

6.5 Mathematical development of temperature model for forward circulation

The mathematical solutions of the counter-current heat exchanger including the following main parts:

1. *Dimensionless time function*
2. *Overall heat-transfer coefficient*
3. *Heat flow from the formation to the annulus*
4. *General solution of the circulating mud temperature*

6.5.1 Dimensionless time function

A dimensionless time function is necessary to consider for applying the formation / casing heat conduction. $f(t_D)$ shows how the transient heat flow from the formation to the wellbore changes with time. This time function depends on the conditions specified for heat conduction. For uniform heat flux, cylindrical-source well, the Hasan and Kabir proposed the following expressions:

$$f(t_D) = (1.1281\sqrt{t_D}) * (1 - 0.3\sqrt{t_D}) \quad (6.1)$$

If $10^{-10} \leq \quad t_D \leq 1.5$

$$f(t_D) = (0.4063 + 0.5lnt_D) * (1 + \frac{0.6}{t_D}) \quad (6.2)$$

If $t_D > 1.5$

$f(t_D)$ behaviors differently with different t_D boundaries. $f(t_D)$ is proportional to the square root of the t_D when t_D is small, when t_D is large , $f(t_D)$ is log-linear with t_D.

The time function introduced describes the temperature distribution in the formation. Hasan and Kabir method is adopted due to its engineering accuracy.

The dimensionless time, t_D, is expressed by

$$t_D = \frac{\alpha_h t}{{r_c}^2} * 3600 \quad (6.3)$$

Where

$$t = circulation\ time, hr$$

As the circulation time is commonly measured in hours, thus it is necessary to use the number 3600 to avoid discrepancies in the unit conversion.

The thermal diffusivity is giving as:

$$\alpha_h = \frac{k_f}{\rho_{f*}c_f} \quad (6.4)$$

Where

$c_f = specific\ heat\ of\ formation, J/kg\,.℃$,

$\rho_f = density\ of\ formation, kg/m^3$,

$k_f = thermal\ conductivity\ of\ formation, W/(m℃)$, [1]

In general, the thermal conductivity is extremely temperature dependent. The numerical value of the thermal conductivity k_f shows how fast heat will flow in a specified material. The larger the value of thermal diffusivity of the material, the faster heat will diffuse through the given material. [57]

6.5.2 Overall heat-transfer coefficient

The overall heat-transfer coefficient, U_d and U_a, depends on the net resistance to heat flow provided by the fluid inside the tubing, annular fluids, solids, and the casing wall. This overall heat-transfer coefficient can be used to describe the heat transfer from the system to surrounding environment. The value of the overall heat transfer coefficient is assumed to be constant in this study, but in reality it changes with respect to time. [58]

Consider the expression for the heat transfer coefficient for a tubing-annulus system:

$$U_t = \frac{1}{\frac{1}{h_t}+\frac{A_i \ln(r_o/r_i)}{2\pi k_t L}+\frac{A_i}{A_o h_a}} \qquad (6.5)$$

Where

$r_i = inside\ of\ tubing\ radius, m,$

$r_o = outside\ of\ tubing\ radius, m,$

$A_i = area\ of\ the\ inside\ of\ inner\ tube, m^2,$

$A_o = area\ of\ the\ outside\ of\ inner\ tube, m^2,$

$h_t = convection\ heat - transfer\ coefficient\ in\ the\ tubing,$

$h_a = convection\ heat - transfer\ coefficient\ in\ the\ annulus,$

In this temperature model which introduced by Erik Kårstad, the overall heat-transfer coefficient is simplified by assuming $r_i = r_o$, $A_i = A_o$ and $h_a = \ h_a = h_{mud}$ the following relationship is obtained:

$$U_t = \frac{h_{mud}}{2} \qquad (6.6)$$

Then, make two more assumptions: first; infinite conductivity in the earth (i.e.$k_e = \infty$), second; there is no convective heat transfer in the earth (i.e.$h_e = 0$), thus

$$U_a = h_{mud} \qquad (6.7)$$

Finally, we obtain

$U_a = 2U_t$ (6.8)

Where

$h_{mud} = convection\ heat - transfer\ coefficient\ for\ mud,$

$U_a = annular\ heat - transfer\ coefficient, m/(Tt^3), W/(m^2 \cdot ℃),$

$U_t = heat - transfer\ coefficient\ in\ the\ tubing, m/(Tt^3), W/(m^2 \cdot ℃)$

[1]

6.5.3 Heat flow from the formation to the annulus

There is an energy transfer from the high-temperature area to the low-temperature area when a temperature gradient occur in a material body.

The transfer of heat by conduction is proportional to the normal temperature gradient. Due to difference between fluid and geothermal temperatures, there is heat transferring between pumped down fluids, casing and the formation. For an incompressible liquid pumping vertically in a constant-diameter wellbore, the heat conduction equation from or to the wellbore may be expressed as:

$q_f = \frac{2\pi k_f}{f(t_D)} (T_f - T_{wb})dz$ (6.9)

Where

$A = a\ time\ function,$

$z = depth\ below\ surface, meters,$

$k_f = thermal\ conductivity\ of\ earth, W/(m℃),$

$q_f = heat\ flow\ from\ formation\ to\ annulus, kJ,$

$T_{wb} = the\ wellbore/formation\ interface\ temperature, ℃$

In this study, forward circulation scenario is presented since it is the norm. [1]

The temperature effects in the well has no doubt an important role in evaluating of wellbore pressure. This effect result in change in density of mud, and as well as viscosity. High temperature leads to expansion of fluid in the wellbore, while high pressure causes compression of fluid in deep wells. Hence, a good understanding of the impacts is important to improve the accuracy on estimation of bottom hole pressure during MPD operations. [56]

Temperature increases with depth. As the density of the fluid decreases with increasing temperature, the more denser cold fluid displaces the less dense warm fluid and therefore a convection current is established inside the well. [1]

The figure simulates fluid temperature as function of depth and circulation time for a forward circulation in a 4800 meters deep well. It shows the temperatures in the drillpipe and annulus increase with increasing geothermal temperature in the formation. T_d is drill pipe/tubing temperature, T_a is annular fluid temperature and T_f represents undisturbed earth temperature that exists in the formation before drilling operation starts. A nearly constant temperature difference between the annulus and drillpipe is set up immediately after fluid passes 1000meters depth and maintained until it reaches the max temperature near the bottom of the hole in the circulation process. As figure shows, the annular and drillstem mud temperature are identical at the bottom of the well. Illustration shows $T_d < T_a$ because of the drill string is assumed as a counter-current heat exchanger in the simulated well, this is discussed earlier in section 6.4. The prediction from the temperature model was used to estimate density profile downhole by means of a density model. Assuming isobaric condition, increasing temperature will result in reduction of density downhole. [1]

Bottom hole fluid temperature is continually changes with depth.

The fig. 19 evident the density of drilling fluid decreases with increasing temperature in the same well. The lowest mud density in the annulus appears approximately at a point where the max temperature obtained in the well.

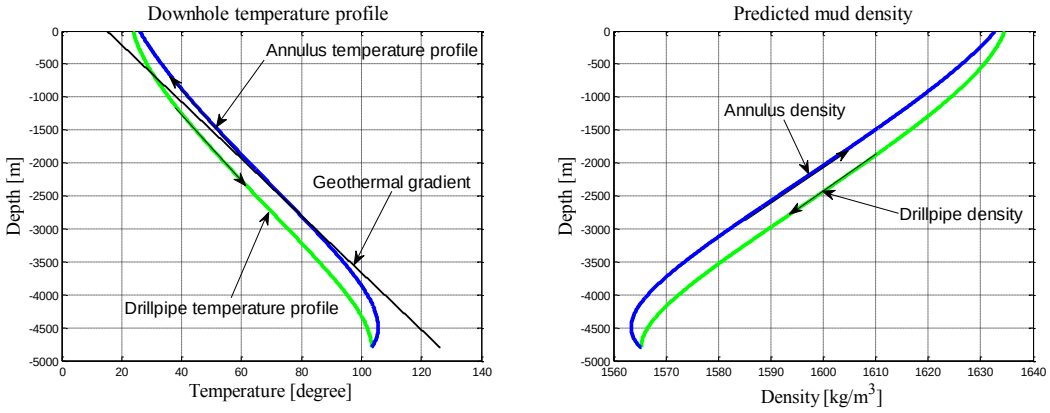

Figure 19: Illustration of downhole temperature and density

In order to design optimal drilling fluid density and choke size, perfect evaluation of predictable pressure along the wellbore is essential in MPD. In turn, estimation of pressure requires accurate information on temperature behavior along the wellbore. [59]

Experimental results in [59] evident that, the density behavior of slightly compressible fluids under low pressures is affected more by temperature than by pressure, an increase in temperature may provide a considerably reduction on density of the drilling fluid. [59]

6.5.4 General solution of the circulating mud temperature

Considering an elemental section of the drillstring, and with heat transfer rate(q_d), the drillstring absorbs heat at depth z, while that of the annulus (q_a) is at z+dz.

In a similar vein, the heat transfer by conduction between the drillstring(q_{ad}), the annulus and the formation(q_f).

The energy balance is giving by the following relationships

$$q_d(z) - q_d(z+dz) = -q_{ad} \quad (6.10)$$

$$q_a(z+dz) - q_a(z) = q_{ad} - q_f \quad (6.11)$$

Where

$$q_d(z) = wC_{fl}T_p(z) \quad (6.12)$$

$$q_a(z) = wC_{fl}T_a(z) \quad (6.13)$$

$$q_{ad} = 2\pi\, r_d\, U_d(T_a - T_d)dz \quad (6.14)$$

$$q_f = 2\pi\, r_c\, U_a(T_{wb} - T_a)dz \quad (6.15)$$

$w = mass\ flow\ rate\ of\ fluid, kg/s,$

$q_d = convective\ heat\ flow\ in\ the\ drill\ string, mL^2/t^3, kJ,$

$q_a = convective\ heat\ flow\ in\ annulus, mL^2/t^3, kJ,$

$q_{ad} = heat\ flow\ from\ annulus\ to\ drill\ string, mL^2/t^3, kJ,$

$q_f = heat\ flow\ from\ formation\ to\ annulus, mL^2/t^3, kJ,$

$T_a = annular\ fluid\ temperature, ℃,$

$T_d = tubing\ fluid\ temperatuer, ℃,$

Combing equations (6.9) and (6.15) yields the following equation for the heat conduction between the annulus and the formation

$$q_f = \frac{2\pi\, r_c\, U_a k_f}{w(k_f + r_c\, U_a\, f(t_D))} * (T_f - T_a)dz \quad (6.16)$$

By rearrange equations (6.12)-(6.16), equations (6.10) and (6.11) then take the form

$$T_a = T_d + B\frac{dTd}{dz} \quad (6.17)$$

$$A\frac{dTa}{dz} = (T_a - T_d) * \frac{A}{B} - (T_f - T_a) \quad (6.18)$$

Where

$$A = \frac{wC_{fl}}{2\pi r_c\, U_a} * (1 + \frac{r_c\, U_a\, f(t_D)}{k_f}) \quad (6.19)$$

$$B = \frac{wC_{fl}}{2\pi r_d\, U_d} \quad (6.20)$$

In this study, the formation temperature or geothermal temperature, T_f, is assumed as a linear function of depth,

$$T_f(z) = T_{sf} + gG * z \quad (6.21)$$

Where

$T_{sf} = surface\ temperature$, ℃,

$gG = geothermal\ gradient, T/L$, ℃$/m$,

$z = depth\ of\ the\ well$

Combine Eqs.(6.17),(6.18) and (6.21) the following Eq is obtained

$$AB\frac{dT_d^2}{dz^2} - B\frac{dT_d}{dz} - T_d + T_{sf} + gGz = 0 \quad (6.22)$$

Assuming initial boundary conditions

$T_d = T_{in}$ at $z = 0$, at the wellhead (6.23)

and

$T_d = T_a$ at $z = D$, at the bottomhole (6.24)

After the boundary conditions are employed, the general solution of the counter-current heat exchange with respect to forward circulation in a circulating well can be found as follows

$$T_d(z,t) = \alpha * e^{\lambda_1 z} + \beta * e^{\lambda_2 z} + gG * z - B * gZ + T_{sf} \quad (6.25)$$

$$T_d(z,t) = (1 + \lambda_1 B) * \alpha * e^{\lambda_1 z} + (1 + \lambda_2 B) * \beta * e^{\lambda_2 z} + gG * z + T_{sf} \quad (6.26)$$

Where

$$\lambda_1 = \frac{1}{2A}\,(1 - \sqrt{1 + \frac{4A}{B}}) \quad (6.27)$$

$$\lambda_2 = \frac{1}{2A}\,(1 + \sqrt{1 + \frac{4A}{B}}) \quad (6.28)$$

$$\alpha = -\frac{(T_{in} + B*gG - T_{sf})*\lambda_2 e^{\lambda_2 D} + gG}{\lambda_1 e^{\lambda_1 D} - \lambda_2 e^{\lambda_2 D}} \quad (6.29)$$

$$\beta = \frac{(T_{in} + B*gG - T_{sf})*\lambda_1 e^{\lambda_1 D} + gG}{\lambda_1 e^{\lambda_1 D} - \lambda_2 e^{\lambda_2 D}} \quad (6.30)$$

Tubular fluid temperature (T_a) and tubing fluid temperature (T_d) are depth and time dependent. [1]

7 Case studies

7.1 Case study 1

Sensitivity analysis on downhole temperature and mud density prediction during forward circulation

Temperature simulations were performed for different factors that influence on downhole pressure directly or indirectly for forward circulation.

Sensitivity analysis is carried out by study temperature curves with a range of different variables. There are many variables that play a part in the influencing of downhole temperature behavior during circulation. Variables that selected for this sensitivity analysis are:

1. Circulation time
2. Overall heat transfer coefficient
3. Circulation rate
4. Heat capacity of fluid/fluid heat capacity
5. Wellbore geometry
6. Fluid inlet temperature

The temperature profile makes it possible to predict density. By coupling the temperature behavior into the density model, the density profile downhole is modelled. Note that the pressure is not varying (under isobaric condition), it is calculated as an average value of surface and hydrostatic pressure. This was described in the temperature model section.

Temperature and pressure have different influences on densities of oil based and water based drilling fluid. In general, for the same fluids (same weight), the density of a water based fluid is lower than that of an oil based drilling fluid at high temperature and high pressure condition. It is verified by experiment data (see, for example, W.C.McMordie Jr. et al.(1982). [60] However, incompressible drilling fluid is used here.

Density is impacted directly by downhole variations in temperature and pressure, the drilling fluid at any depth experiences two opposite effects. Density of the drilling fluid affects the rate of penetration in contrary way. During drilling, in order to maintain wellbore stability and well control, higher mud density is needed. [61]

It is important to note that the following density curves are for illustration purpose only and they are valid for the particular set of conditions to produce those results. What parameters are important for the density determination will vary with downhole environment.

Each of the simulations change one variable at a time, the output from the model was found significantly different.

7.1.1 Circulation time

The plot of Depth vs Temperature is shown in fig.20.

The fig. 20 illustrates a forward circulation. Three simulations compare downhole temperature profiles at three different circulation time after 0.02 hour, 2 hours and 15 hours of circulation, respectively.

Max downhole temperature changes from 112 degrees to 98.9599 degrees when circulation time increases from 0.02 hours to 2 hours in the well.

As it mentioned in the temperature model section, if the well has ceased for some time, it appears reasonable to assume a linear increase in temperature with depth.

The temperature profiles at the lower part of the well are deflecting more from the geothermal gradient curve with longer circulation times. The maximum fluid temperature tends to move up in the annulus as circulation time increases. The figure illustrates the maximum temperature after 0.02 hours of circulation was approximately 14degrees higher than after 15 hours of circulation in the system and the location of the maximum temperature moved up122 meters.

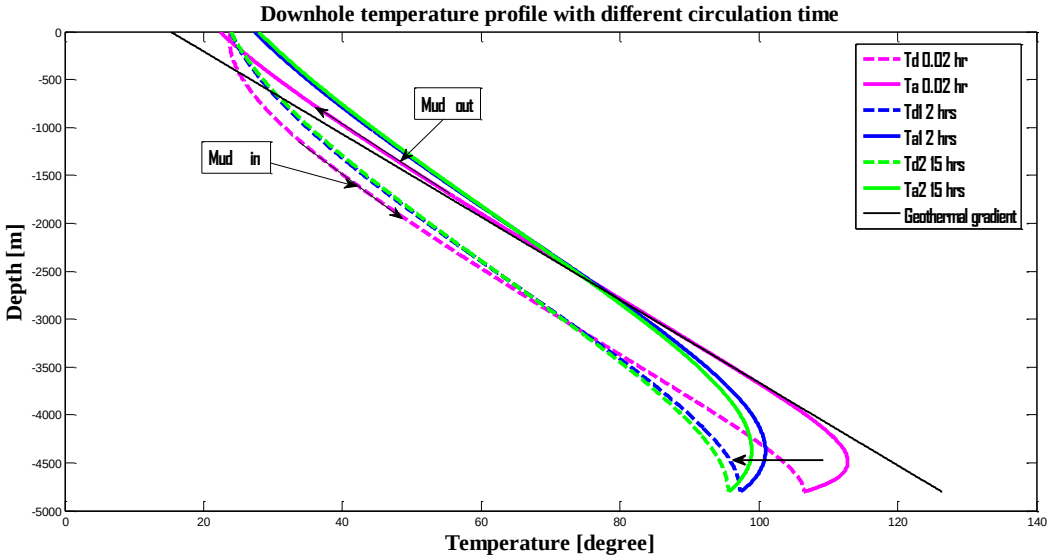

Figure 20: Effect of different circulation times on the temperature behavior in annular and drillpipe during circulation.

Table 4 summarizes the inlet mud temperature at surface, return mud temperature at surface, temperatures at bit, maximum temperature and at what depth the maximum temperatures are located for different circulation times.

Table 4 Simulation results of downhole temperature profile for different circulation times

Circulation Time $[hours]$	Temperature At bit [°C]	Maximum Temperature [°C]	Max Temp at $[m]$	Inlet Mud temperature at surface [°C]	Return Mud temperature at surface [°C]
0.02	106.4561	112.81	4486	23.89	22.34
2	93.3070	100.94	4366	23.89	27.35
15	95.61	98.9599	4364	23.89	27.95

Figure 21 shows the plot of Depth vs Density.

By coupling the values found in the foregoing temperature model into the density model mentioned in section 4, a density profile is developed in the simulated well as the curves shown in the fig. 21. The results indicate that a higher value of temperature of drillpipe and annulus from the surface to drill bit, leads to lower density at an identical trip. Density is having a minimal value in the annulus at 0.02 hour circulation scenario. The fluid density increases as circulation time increases, the reason is continuously cooling of the well when circulates in larger times.

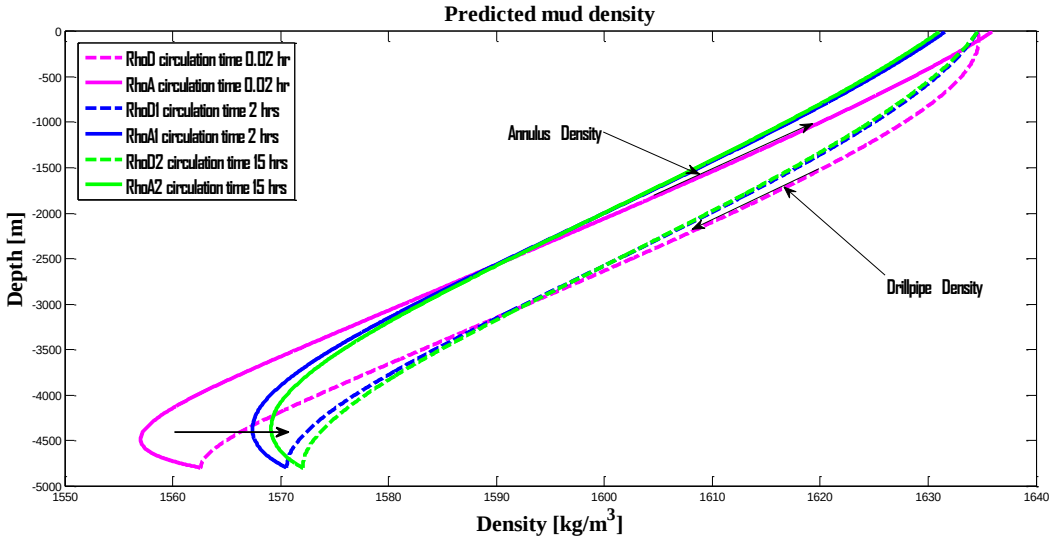

Figure 21: Effect of different circulation times on the density in the annulus and drillpipe during circulation under isobaric condition.

Table 5 summarizes the mud density at surface condition, at bottomhole, density difference between surface and bottomhole, the lowest the density and at what depth the lowest densities are located for different circulation times.

Table 5 Simulation results of downhole density profile for different circulation times

Circulation Time $[hours]$	Mud In density at surface $\left[\frac{kg}{m^3}\right]$	Mud Density at bottomhole $\left[\frac{kg}{m^3}\right]$	Difference Between surface and bottomhole $\left[\frac{kg}{m^3}\right]$	Lowest Density $\left[\frac{kg}{m^3}\right]$	Lowest Density at depth $[m]$
0.02	1634.6	1562.6	72	1557.0	4486
2	1634.6	1570.6	64	1567.4	4366
15	1634.6	1572.0	62.6	1569.1	4364

7.1.2 Overall heat-transfer coefficient

Fig. 22 summarizes how three varying conditions influences the temperature down hole.

The temperature curve becomes narrow by selecting$U_a = U_d$, the value of T_d is strongly increased. Temperature in drillpipe is lowest by selecting $U_a = 2U_d$ while it is highest by choosing $U_a = U_d$.

The wellbore temperature is almost insensitive to three pairs of randomly selected U values. There is only a small difference among them at the lower part of the hole. Heat transmission is also relatively weaken between return fluids and surrounding formation.

It is obvious that selection of the same U (green curves) has effect of another class on annular and drillpipe mud temperature compare with the other two curves.

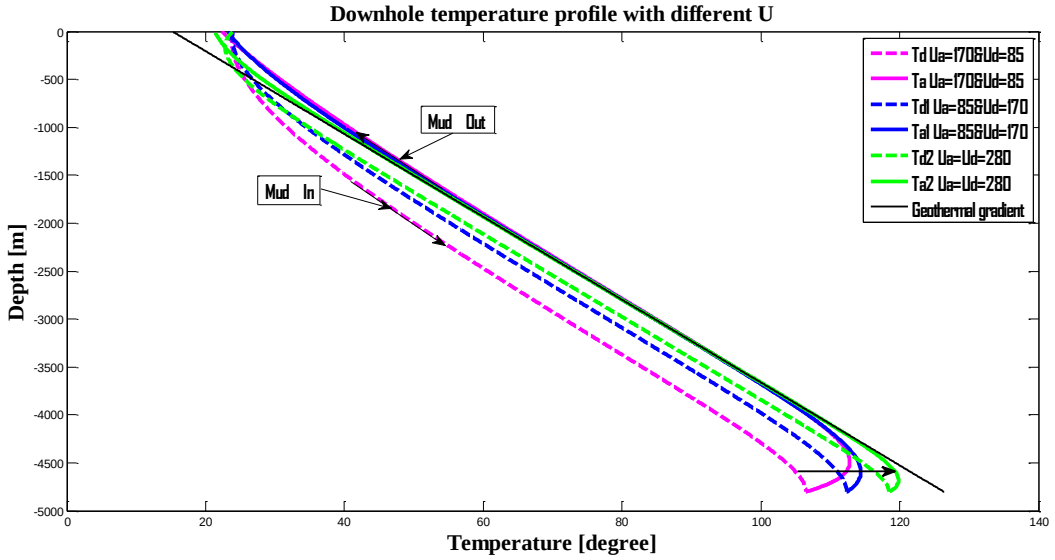

Figure 22: Effect of different U on the temperature behavior in annular and drillpipe during circulation.

The following table summarizes the mud temperature at surface, return mud temperature at surface, temperatures at bit, maximum temperature and at what depth the maximum temperatures are located for different U.

Table 6 Simulation results of downhole temperature profile for different U

U	Temperature At Bit [℃]	Maximum Temperature [℃]	Max Temp at $[m]$	Inlet Mud temperature at surface [℃]	Return Mud temperature at surface [℃]
$U_a = 170, U_d = 85$	106.4561	112.81	4486	23.89	22.34
$U_a = 250, U_d = 125$	112.3664	114.40	4585	23.89	23.19
$U_a = U_d = 280$	118.4719	119.83	4550	23.89	21.34

Fig. 23 illustrates when $U_a = U_d = 280$, the almost parallel density in annulus, ρ_a and density in drillpipe ρ_d curves shrink to one third of the size compared to choose initial U values ($U_a = 170$ and $U_d = 85$). Density profile shows that when selecting $U_a = 2U_d$, the system produces the highest the density at the bottomhole.

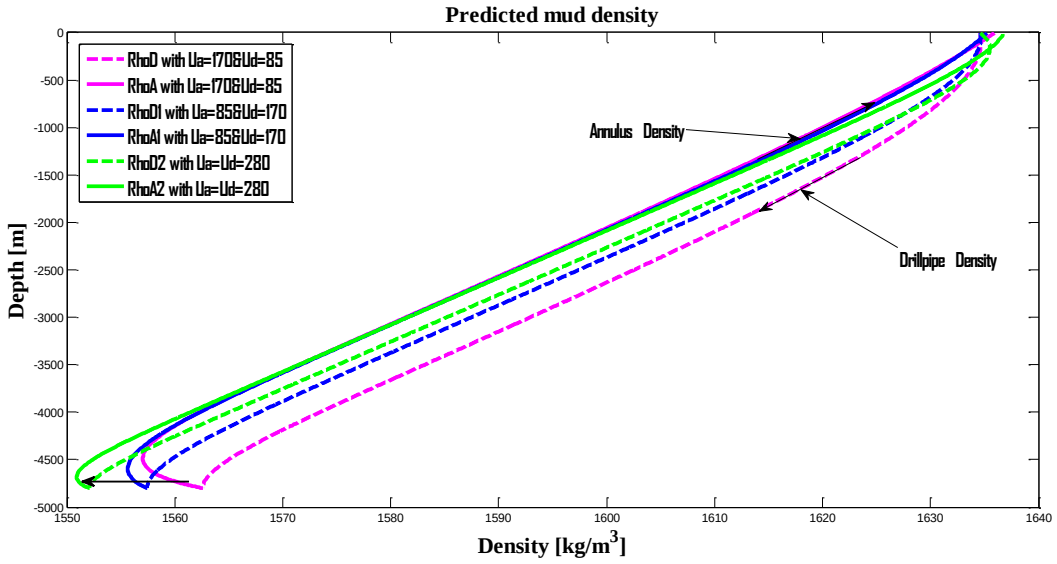

Figure 23: Effect of different U on the density in the annulus and drillpipe during circulation under isobaric condition.

Table 7 summarizes the mud in density at surface, at bottomhole, density difference between surface and bottomhole, the lowest the density and at what depth the lowest densities are located for different U values.

Table 7 Simulation results of downhole density profile for different *U*

U	Mud In density at surface $\left[\frac{kg}{m^3}\right]$	Mud Density at bottomhole $\left[\frac{kg}{m^3}\right]$	Difference between surface and bottomhole $\left[\frac{kg}{m^3}\right]$	Lowest Density $\left[\frac{kg}{m^3}\right]$	Lowest Density at depth $[m]$
$U_a = 170, U_d = 85$	1634.6	1562.6	72	1557.0	4486
$U_a = 250, U_d = 125$	1634.6	1557.4	77.2	1555.7	4585
$U_a = U_d = 280$	1634.6	1552.1	82.5	1550.9	4550

7.1.3 Circulation rate

Higher rates create lower bottomhole temperatures. When drilling in a high temperature well, lower bottomhole temperature can contributes to a reduction in downhole tools failures, so potentially preventing tripping for changing damaged tools. [32]

Drilling fluid temperature is always in a transient condition and strongly affected by circulation rate. With high flow rate gives better hole cleaning in the hole and torque and drag effect are reduced, it contributes to improved transmission of weight to the bit. [32]

The fig. 24 shows a comparison of temperature results from three different circulation rates. With increasing flow rate, temperatures are reduced by a significant amount.

In this simulation, fig. 24 is shown the drill-pipe and annular fluid temperature profiles at three different circulation rates ranging from 47.696 to 108m^3/hr. Fluid temperature is strongly sensitive to the flow rate. At flow rate of 47.6964m^3/hr, the circulating fluid in the annulus is in relative agreement with the surrounding formation temperature, but at higher rates, the temperature of return fluids in the annulus change faster away from the undisturbed temperature. The higher circulation rates lead to lower temperature distribution and result in increased disparity between T_a and T_d,which occurs after the system reaches 500 meters.

The bottomhole temperature is greater for the lower rate. However, for an increase in flow rate from 95.3938m^3/hr to 108m^3/hr, the temperature at bit lowered only 3.8 degrees.

The location of the maximum temperature point is also dependent on circulating rate, it moves continuously up the annulus as circulating rate increases because circulation cools down the annulus.

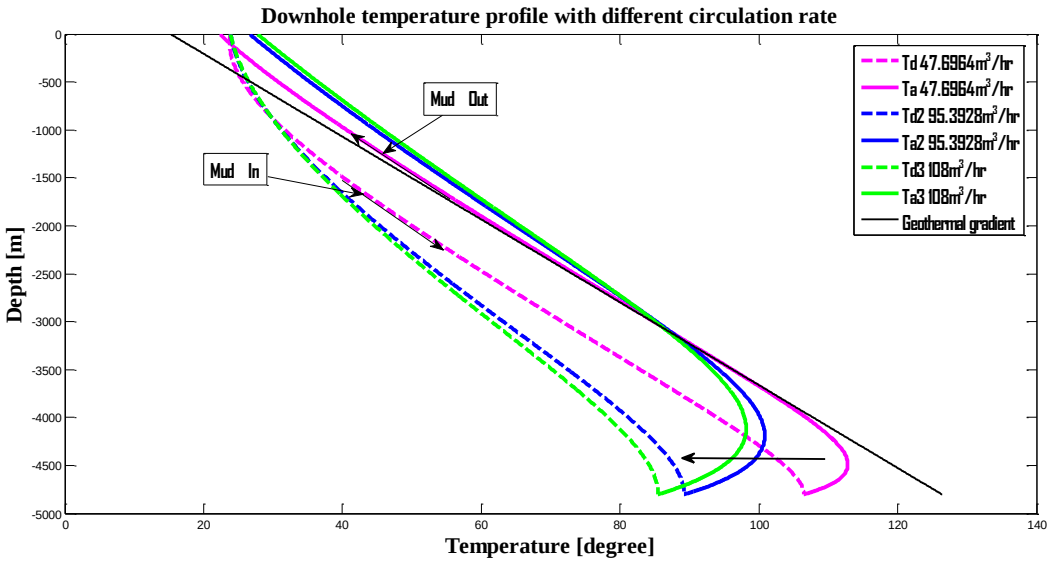

Figure 24: Effect of different circulation rates on the temperature behavior in annular and drillpipe during circulation.

The following table summarizes the inlet mud temperature at surface, return mud temperature at surface, temperatures at bit, maximum temperature and at what depth the maximum temperatures are located for different circulation rates.

Table 8 Simulation results of downhole temperature profile for different circulation rates

Circulation rate $\left[m^3/hr\right]$	Temperature At Bit [°C]	Maximum Temperature [°C]	Max Temp at $[meters]$	Inlet Mud temperature at surface [°C]	Return Mud temperature at surface [°C]
47.6969	106.4561	112.81	4486	23.89	22.34
95.3928	89.2615	100.85	4182	23.89	26.67
108	85.5090	98.1623	4116	23.89	27.80

For density profile:

Fig. 25 shows the fluid density in drillpipe are nearly equal for all three circulation rates at the beginning of the simulation. Increased circulation rate gives higher density at the bottom of the hole.

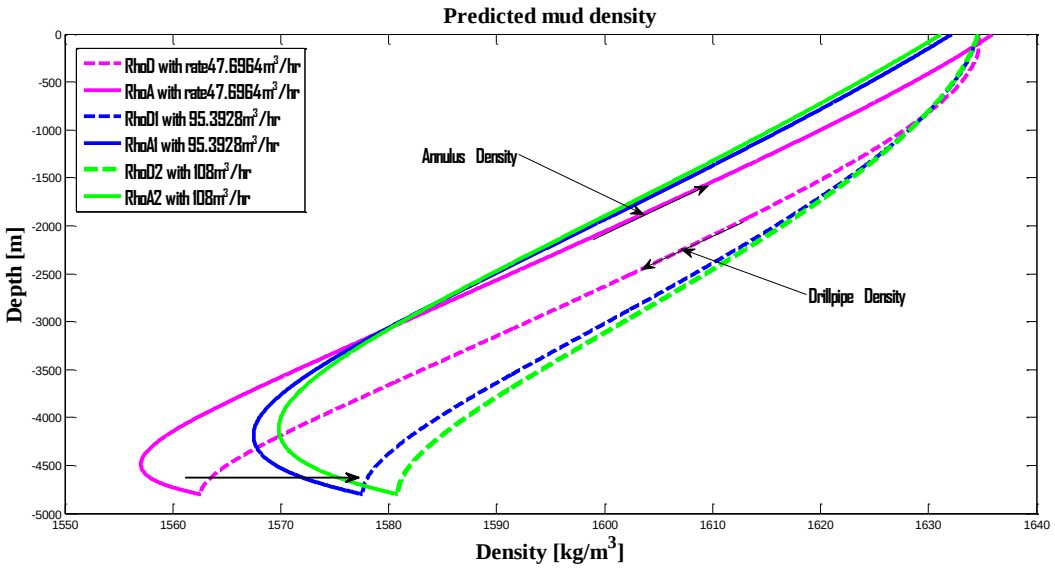

Figure 25: Effect of different circulation rates on the density in annular and drillpipe during circulation under isobaric condition.

When double the circulation rate from 47.6969 to 95.3928, the density changed$15\,\frac{kg}{m^3}$ $\left(\text{from } 72 \text{ to } 57\ \frac{kg}{m^3}\right)$. For the current well means the BHP reduced 7.06 bar $(15 \times g \times 4800m = 7.06)$ due to doubling of circulation rate. This pressure difference is significant when operating in a tight drilling window when pressure gap between pore pressure and formation fracture pressure is less than 100 Pa as it mentioned in the MPD technology section.
It remainders that temperature effect on density should always take into account when planning MPD project.

Table summarizes the mud density at surface condition, at bottomhole, density difference between surface and bottomhole, the lowest the density and at which depth the lowest densities are located for different circulation rates.

Table 9 Simulation results of downhole density profile for different circulation rates

Circulation rate $\left[\frac{m^3}{hr}\right]$	Mud In density at surface $\left[\frac{kg}{m^3}\right]$	Mud Density at bottomhole $\left[\frac{kg}{m^3}\right]$	Difference between surface and bottomhole $\left[\frac{kg}{m^3}\right]$	Lowest Density $\left[\frac{kg}{m^3}\right]$	Lowest Density at depth $[m]$
47.6969	1634.6	1562.6	72	1557.0	4486
95.3928	1634.6	1577.6	57	1567.5	4182
108	1634.6	1580.9	53.7	1569.8	4116

7.1.4 Heat capacity of fluid

These curves in fig. 26 represent the dynamic reaction of the circulating system for different heat capacities.

By selecting a heat capacity with value 1676 J/kg ℃ , the temperature in the drillpipe achieves a path parallel to the annular temperature soon after it runs into the pipe. Fig. 26 shows the wellbore fluid cools the formation from 3430 to 4800 for lower heat capacity value. But when changing to higher heat capacity value, the system cools the formation from 3147 to 4800meter. Nevertheless, surface temperatures for return fluids are not much different (4.3℃).

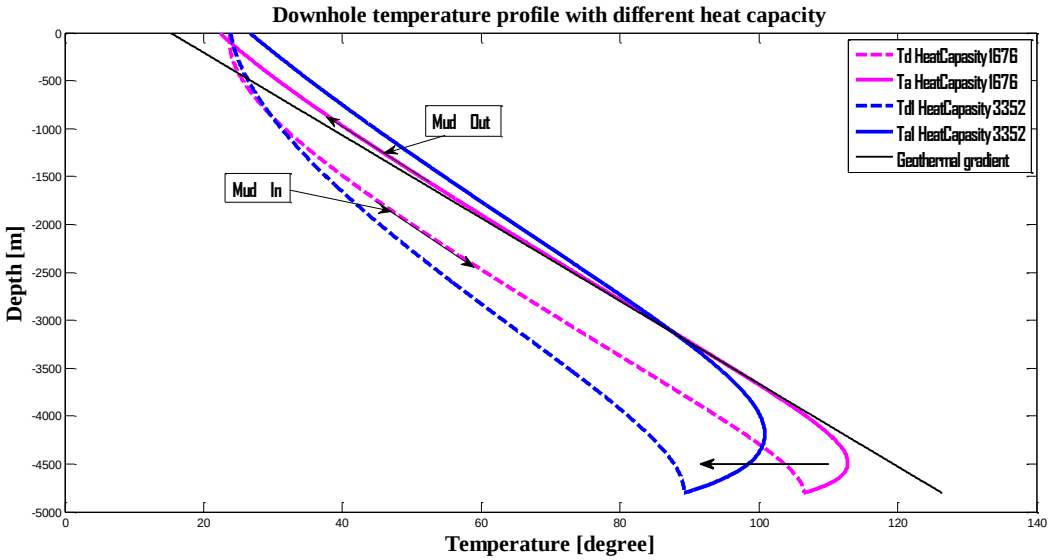

Figure 26: Effect of different heat capacities on the temperature in annular and drillpipe during circulation.

The following table summarizes the inlet mud temperature at surface, return mud temperature at surface, temperatures at bit, maximum temperature and at what depth the maximum temperatures are located for different circulation rates.

Table 10 Simulation results of downhole temperature profile for different heat capacities

Heat capacity J/kg ℃	Temperature At Bit [℃]	Maximum Temperature [℃]	Max Temp at $[meters]$	Inlet Mud temperature at surface [℃]	Return Mud temperature at surface [℃]
1676	108.4561	112.81	4366	23.89	22.34
3352	89.2615	100.85	4196	23.89	26.67

Fig. 27 shows that the higher heat capacity results in increased parallel gap between ρ_a and ρ_d. When the heat capacity is doubled, the density differences between surface condition and bottomhole changed$15\,\frac{kg}{m^3}$ $\left(\text{from } 72 \text{ to } 57\ \frac{kg}{m^3}\right)$, this result is perfectly agree with the result when doubling of circulation rates. The bottomhole pressure decreased $7.06\ bar$ $(15 \times g \times 4800m = 7.06)$ due to doubling of heat capacity change.

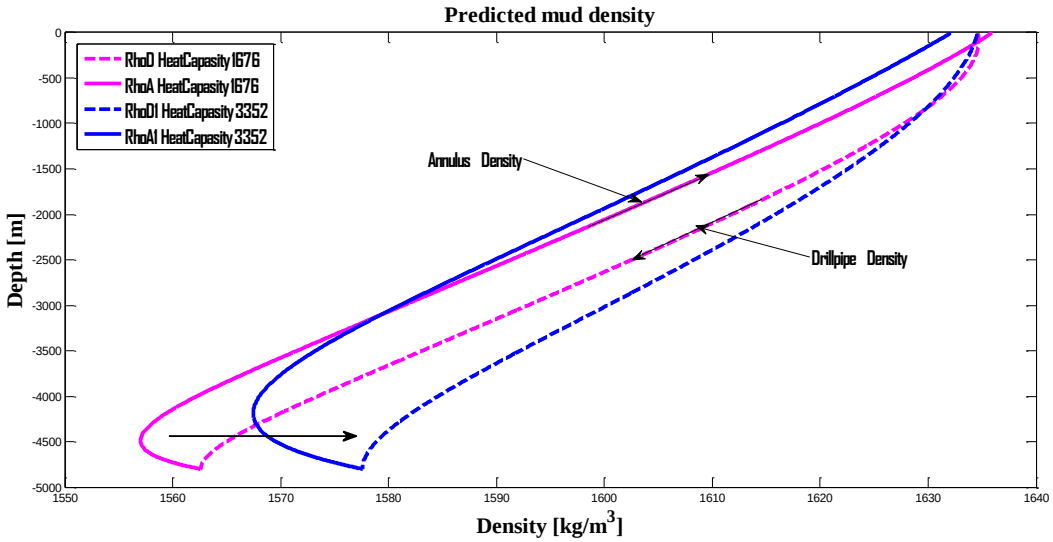

Figure 27: Effect of different mud heat capacities on the density in annular and drillpipe during circulation under isobaric condition.

Table 10 summarizes the mud density at surface condition, at bottomhole, density difference between surface and bottomhole, the lowest density and at which depth the lowest densities are located for different heat capacities.

Table 11 Simulation results of downhole density profile for different heat capacities

Heat capacity J/kg ℃	Mud In density at surface $\left[\frac{kg}{m^3}\right]$	Mud Density at bottomhole $\left[\frac{kg}{m^3}\right]$	Difference Between surface and bottomhole $\left[\frac{kg}{m^3}\right]$	Lowest Density $\left[\frac{kg}{m^3}\right]$	Lowest Density at depth $[m]$
1676	1634.6	1562.6	72	1557.0	4366
3352	1634.6	1577.6	57	1567.5	4196

7.1.5 Geometry effect

Fig. 28 shows curves of temperature distribution in drillpipe and annulus when regarding two different geometries of the hole. A slim hole results in broader distance between the T_a and T_d

after the fluid reaches below roughly 1000 meter depth. It is also observed that there is a small extent temperature change for return fluids at the surface for two different geometries.
The bottomhole temperature for slim hole is slightly cooler. By selecting a slim hole, the system cools the formation longer than larger hole.

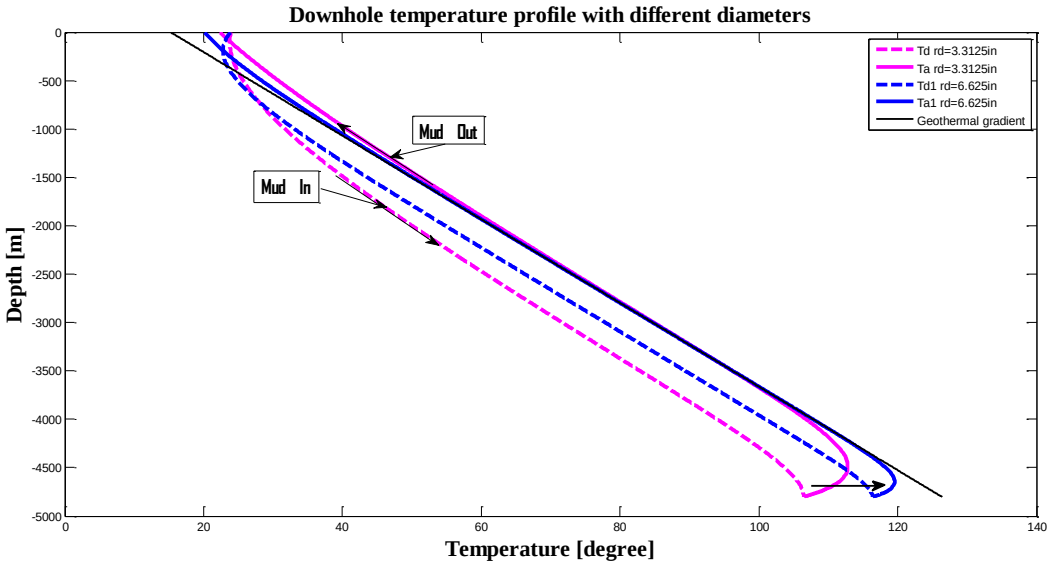

Figure 28: Effect of different geometries on the temperature behavior in annular and drillpipe during circulation.

Table 12 summarizes the inlet mud temperature at surface, return mud temperature at surface, temperatures at bit, maximum temperature and at which depth the maximum temperatures are located for different hole sizes.

Table 12 Simulation results of downhole temperature profile for different geometries

Drillstem outer radius $[in]$	Temperature At Bit [°C]	Maximum Temperature [°C]	Max Temp at $[m]$	Inlet Mud temperature at surface [°C]	Return Mud temperature at surface [°C]
3.3125	106.4561	112.81	4486	23.89	22.34
6.625	116.3516	119.54	4642	23.89	20.18

Behavior of downhole temperatures with two different geometries for forward circulation are shown in fig. 29. When we enlarge the drillstem reduces the mud density at bottomhole, as a result, decreases the bottomhole pressure. However, it appears only a small deviation at the upper part of the well for annular densities compare two different drillstem sizes.

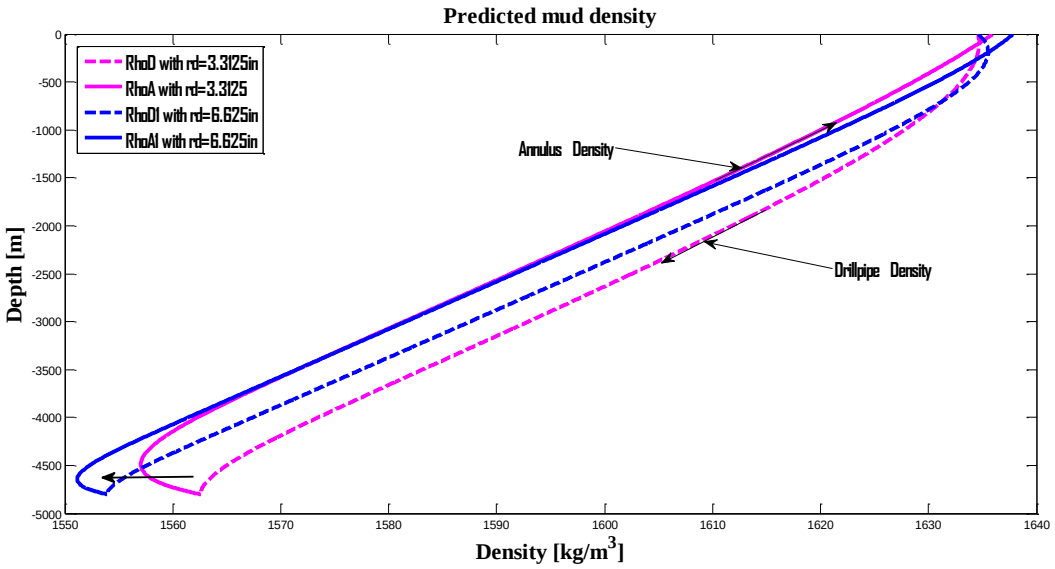

Figure 29: Effect of different geometries on density in the annular and drillpipe during forward circulation under isobaric condition.

The following table summarizes the mud density at surface condition, mud density at bottomhole, density difference between surface and bottomhole, the lowest density and at which depth the lowest densities are located for different drillstem outer radius.

Table 13 Simulation results of downhole density profile for different geometries

Drillstem outer radius $[in]$	Mud In density at surface $\left[\frac{kg}{m^3}\right]$	Mud Density at bottomhole $\left[\frac{kg}{m^3}\right]$	Difference Between surface and bottomhole $\left[\frac{kg}{m^3}\right]$	Lowest Density $\left[\frac{kg}{m^3}\right]$	Lowest Density at depth $[m]$
3.3125	1634.6	1562.6	72	1557.0	4486
6.625	1634.6	1554.0	80.6	1551.2	4642

7.1.6 Inlet fluid temperature

Fig. 30 Illustrates temperature profile for different inlet temperatures.

For different inlet mud temperature system, it effects only the upper part of the well. The temperature behavior at lower part of the well is almost insensitive to inlet temperature at surface condition. Two mud systems have approximately the same temperature profiles both in annular and drillpipe below 3000 meters.

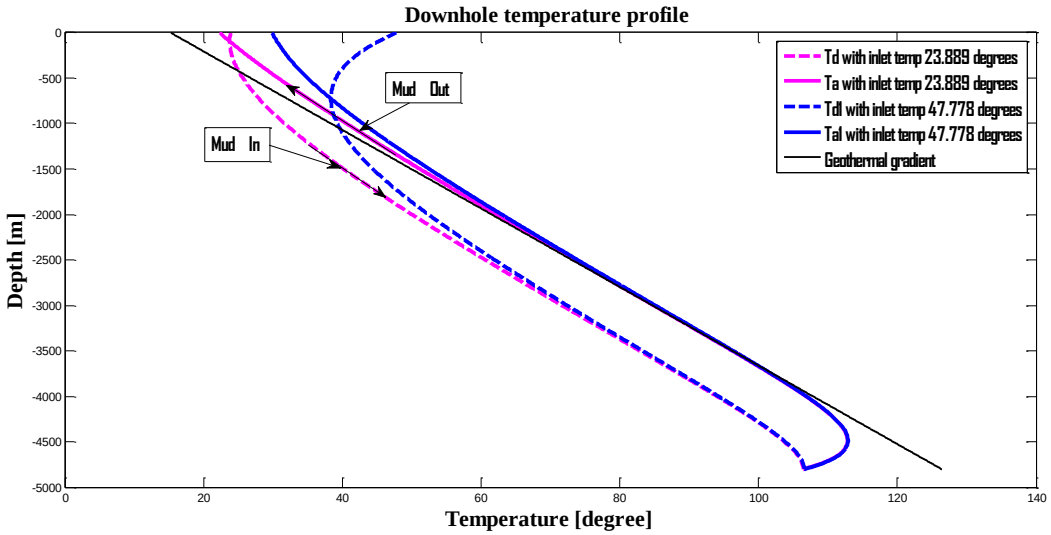

Figure 30: Effect of different inlet temperatures on the temperature in annular and drillpipe during circulation.

Table 14 summarizes the inlet mud temperature and return mud temperature at surface condition, temperatures at bit, maximum temperature and at which depth the maximum temperatures are located for different inlet temperatures.

Table 14 Simulation results of downhole temperature profile for different inlet mud temperatures

Inlet mud temperature [°C]	Temperature At Bit [°C]	Maximum Temperature [°C]	Max Temp at $[m]$	Inlet Mud temperature at surface [°C]	Return Mud temperature at surface [°C]
23.889	106.4561	112.81	4486	23.89	22.34
47.778	106.5792	112.88	4486	47.78	29.89

Fig 31 shows the plot of Depth vs Density

The density of fluid in the drillpipe and annular at lower part of the well are independent of inlet mud temperature at surface conditions. However, higher inlet temperature in shallow well will have more influence on density compare with deep well. The same inlet mud temperatures are simulated in a shallow well, the plot can be seen in the appendix.

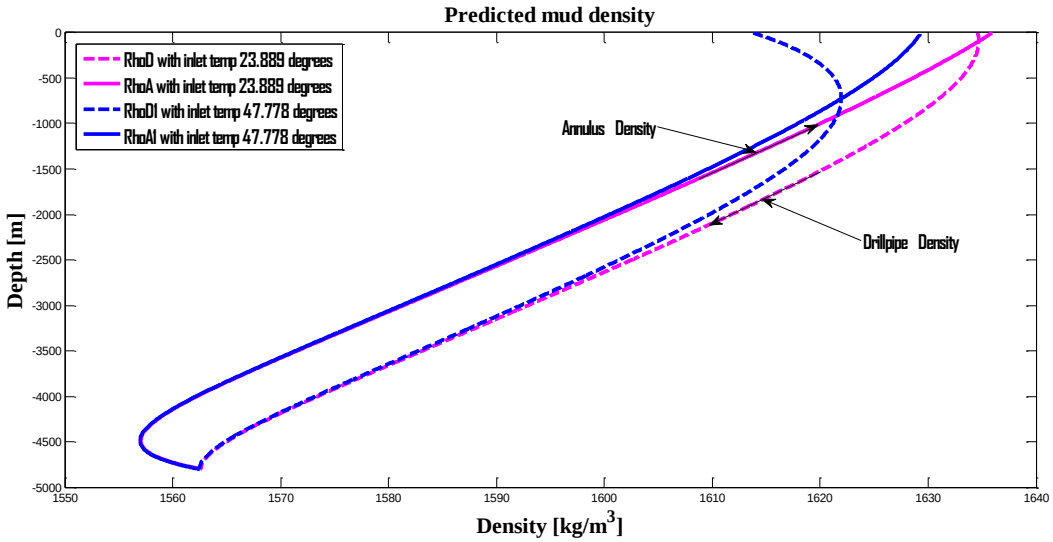

Figure 31: Effect of different inlet temperatures on the density in annular and drillpipe during circulation under isobaric condition.

Table 15 summarizes the mud density at surface condition, at bottomhole, density difference between surface and bottomhol, the lowest density and at which depth the lowest densities are located for different inlet mud temperatures.

Table 15 Simulation results of downhole density profile for different inlet mud temperatures

Inlet mud temperature [℃]	Mud In density at surface $\left[\frac{kg}{m^3}\right]$	Mud Density at bottomhole $\left[\frac{kg}{m^3}\right]$	Difference between surface and bottomhole $\left[\frac{kg}{m^3}\right]$	Lowest Density $\left[\frac{kg}{m^3}\right]$	Lowest Density at depth $[m]$
23.889	1634.6	1562.6	72	1557.0	4486
47.778	1613.8	1562.5	51.3	1557.0	4486

7.2 Conclusions

First of all, those simulations compute the temperature profiles in a forward circulating well. Then taking the temperature effects into consideration and estimate the downhole densities.

In this study, when predicting density profiles in the wells, assumptions that under isobaric conditions (pressure does not change with depth or other parameters) will lead to inaccurate density profiles. This error information might cause well-control problems and negate the beneficial of MPD as the MPD commonly applies to operate in narrow pore and fracture pressure

windows. In some real cases, the pressure margins are only about 30-50 psi. [56] Whether or not a successful MPD operation depends on precise density estimation.

On the basis of the foregoing simulation results, the following conclusions are made:

1. The six different variables influent downhole temperature and density differently, but they interact with one another.
1. The maximum temperature occurs in the annulus, it is slightly higher than the bottomhole temperature for all the variables analyzed.
2. It can be concluded that downhole temperatures are more sensitivity to higher circulation rates and heat capacity changes.
3. The phenome has been observed: higher heat capacity of mud and circulation rates produce the lowest bottomhole temperatures.
4. It found that, higher circulation rate results in higher mud density at the bottomhole, hence, the bottomhole pressure (BHP) will be increased.
5. Higher inlet mud temperature at surface leads to higher return mud temperature at surface, but the temperature behaviors the same as for lower inlet temperature during circulation at the lower part of the well.
6. All the temperature profiles presented here, the lower part of annulus fluid cools the formation as new drilling mud continuously pumping down to the well, in contrast, the upper part of the annulus fluid is transmitted heat by the return fluid flowing up the annulus.
7. The assumed heat capacity is arbitrary, it may lead to uncertainties in the final simulation results.
8. In addition, the overall heat transfer coefficient has been confirmed not to be a constant, but changes with respect to time. [58]
9. Among all the sensitivity analysis being compared, it can be concluded that temperature are more sensitive to changes in circulation rates and the overall heat transfer coefficient compared to those of the other selected variables.

7.3 Future work:

The comparison is not allowable since the true measurement from the well is not available. The output from the models may differ to a certain extent from the reality for some carefully but randomly selected variable under circulation condition. Due to lack of actual field data, some selected value of variables may not be reasonable in reality.

Density could be impact by six different variables, thereby obtain various annular pressure. An overall understanding of the influences of these variables on annular pressure is needed to ensure an ideal design for MPD operations.

The study on the effects of temperature on density is limited with respect to actual data from which assumes constant pressure. However, the mud system in isolation is a complex since it consists many components. A widely understanding of downhole temperature will definitely give an overall picture in order to calculate the downhole pressure. [62]

7.4 Case study 2

7.4.1 Simulation of MPD using BPP during connection.

An implementation of MPD using the BPP has been simulated in order to evaluate BPP MPD performance during connection.

During a joined pipe connection, the standpipe pressure decreases due to shutting down of rig pump. A surface back pressure is applied to compensate the annular friction pressure loss, and controlling influx. [13]When connection is made, pipe tripped out of the hole, rig equipment rechecked, it is important to note that RCD sealing elements must be replaced. [26]

The original MATLAB codes were written by Gerhard Nygaard in 2013. Some modifications have been made after Gerhard Nygaard and [12] to obtain the following simulation effect. The connection is performed by turning off the rig pump. That means the rig pump flow rate is zero during operation.

In order to calculate the mud density, the temperature needs to determine first. How are temperatures in the drillpipe, T_d and temperature in the annulus, T_a are calculated in the simulation?

1. Using temperature model to predict the drillpipe temperature profile for the well;
2. Dividing the well into 4800 boxes since the well is assumed as 4800 meters deep;
3. Sum up the total temperature for those 4800 boxes;
4. Calculate the average temperature for those 4800 points in the drillpipe, the average value represents T_d . Repeat calculation for annulus temperature.

Table 16 Input information that are modified in the simulation

parameters	Values	Description
D_d	$6\frac{5}{8}$ in or 0.168275 m	Drillstem OD
D_c	$8\frac{3}{8}$ in or 0.212725 m	Drill bit size
T_0	20 ℃	Reference temperature
P_0	$9.32 * 10^5$ bar	Reference pressure
ρ_0	1600 $kg/m\text{^}3$	Reference density
α_0	$5.45 * 10^{-4}$	Cubical expansion coefficient of the liquid
β_0	$1.55 * 10^9$ Pa	Isothermal bulk modulus of the liquid
$P_{atomospheric}$	$1.013 * 10^5$ Pa	Atmospheric pressure
T_d	58 ℃	Temperature in drillpipe
$Depth$	1951 meters	The depth of the well

The automated choke was regulated with a PI regulator in this MPD system.

Fig 32: Downhole pressure is shown:

Connection operation occurs in the time interval from 250 to 650 seconds. The Bottomhole pressure is kept precisely at reference level during drilling phase. A pressure fluctuation can be seen just after the initiation of ramping down event, the BHP dropped to 3.265×10^7 Pa. the ramping down process lasted for about 100 seconds. This deviation between reference and measured BHP is caused by friction loss during ramping down the rig pump. By observation, the same oscillations generated shortly after the rig pump ramping down after time=650 seconds. The measured BHP dropped to 3.2825×10^7 Pa. The downhole pressure becomes stable afterwards. Driller starts to restart the drilling operation.

The highest measured pressure spike appears at time=310 seconds which is 6.4 bar ($326.5 - 332.9$). The negative margin of deviation is 6.4 bar. The next pressure spike occurs at 710 seconds and is 4.6 bar ($328.25 - 332.9$). In this simulation, with BPP technology in MPD system the pressure spike that caused by ramping up the rig pump is too high.

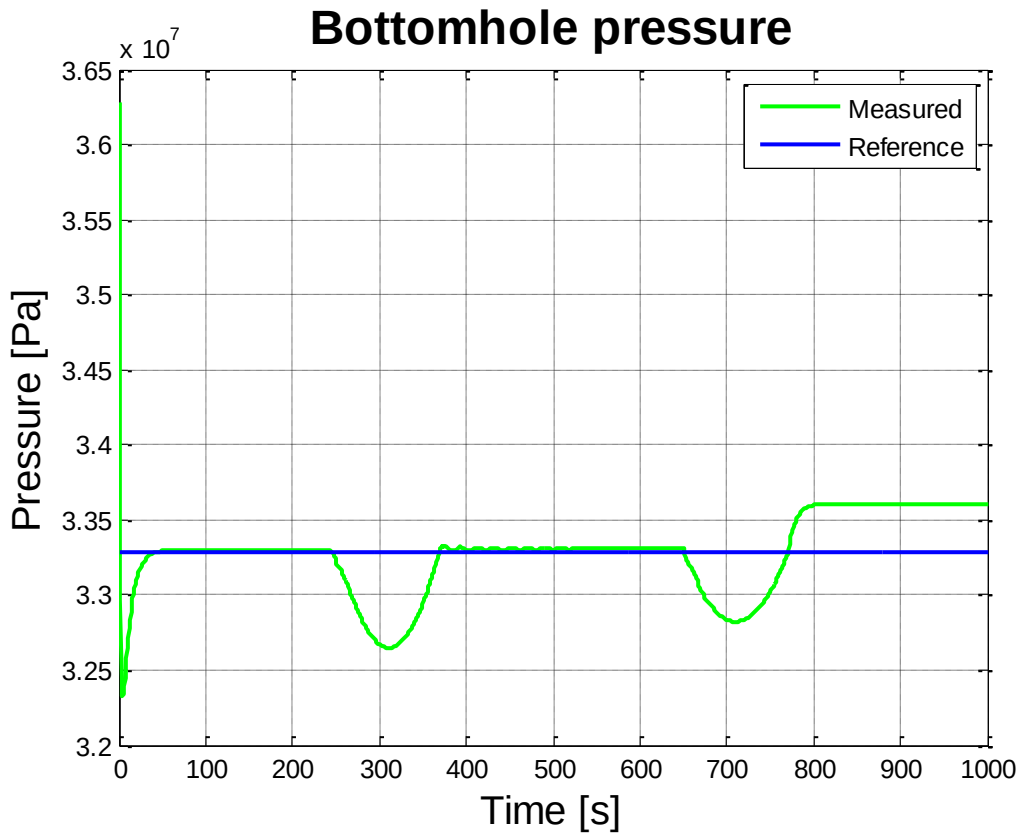

Figure 32: Simulated Bottom hole pressure with BPP method (modified after [12])

The fig. 33 illustrates the pump and choke pressure variation during the connection. Frictional pressure loss is caused by pump pressure in the system. The measured choke pressure follows the set point at all times by contribution of a feed-back control loop including feed-forward terms of disturbance and reference. As is shown in the figure, the choke reference changes and the changes in the pump pressure set point are proximately equal during the connection process. It appears reasonable according to theory in MPD section.

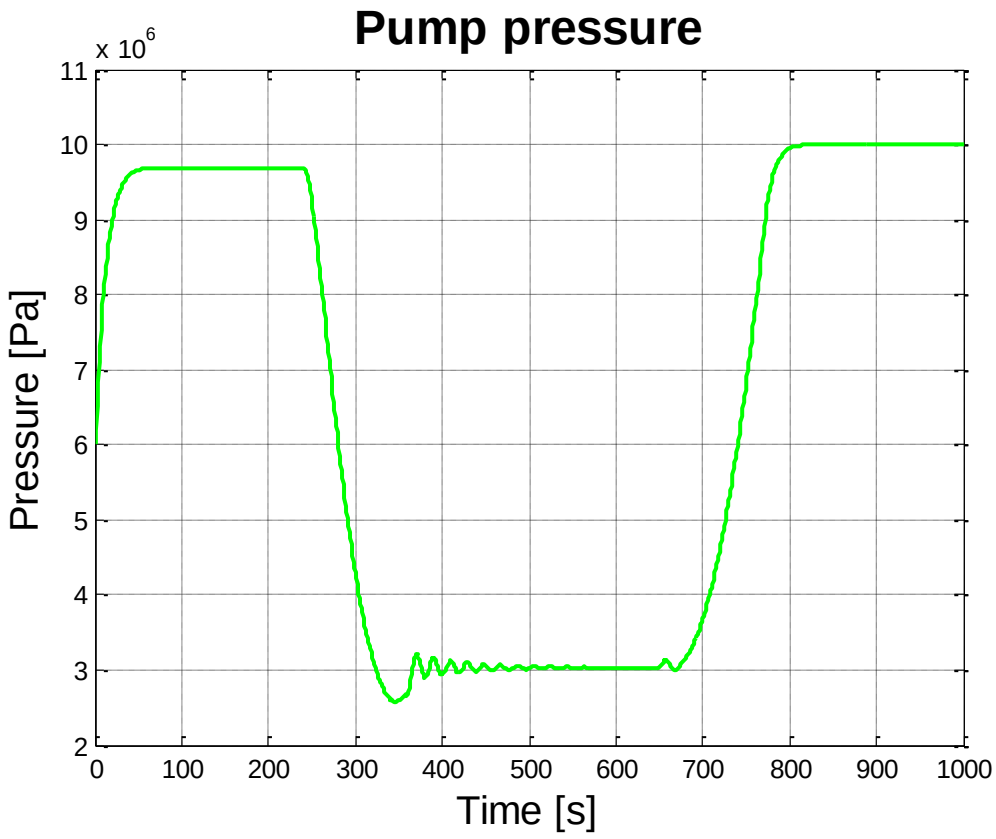

Figure 33: Simulated pump pressure with BPP method (modified after [12])

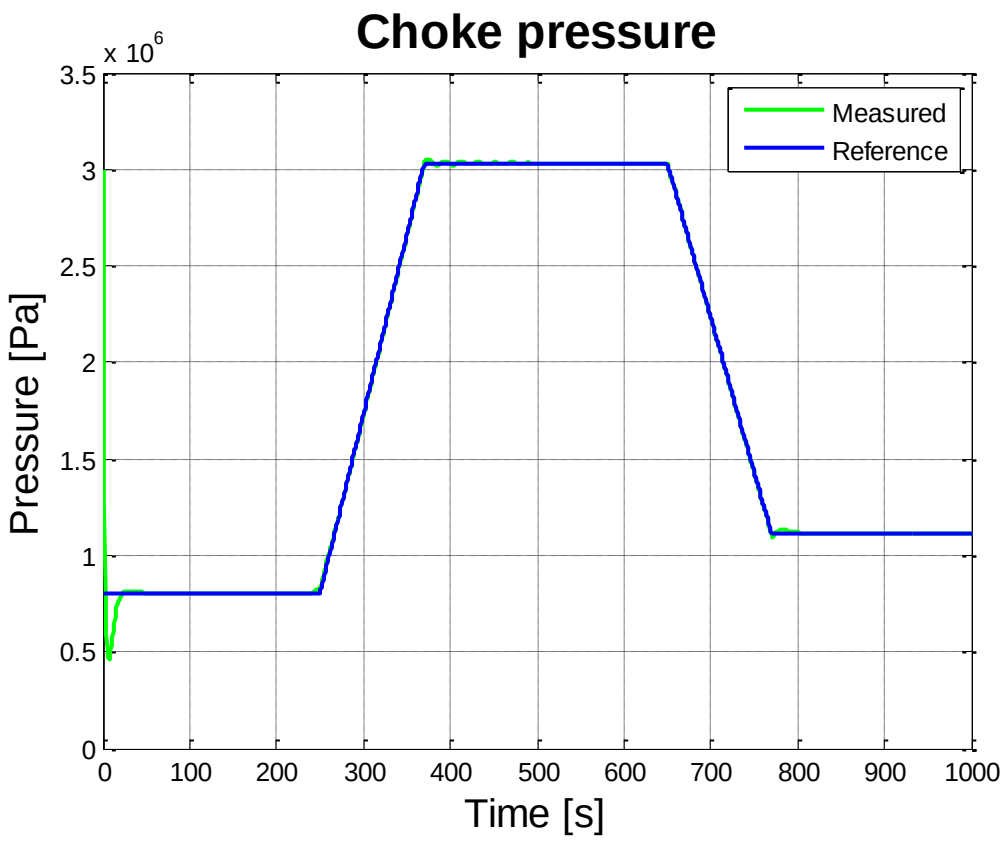

Figure 34: Choke pressure with BPP method (modified after [12])

Fig. 35 Shows the choke position. As the rig pump shuts down, the choke receives signal from control system that the BHP decreases, hence, the choke automatically moves closer to closed position to build up a choke pressure in order to compensate the frictional loss caused by shutting down the rig pump. Thereby maintain a constant BHP. The control system controls the choke position relatively smooth since it does not show any high peak values of the choke opening during the connection.

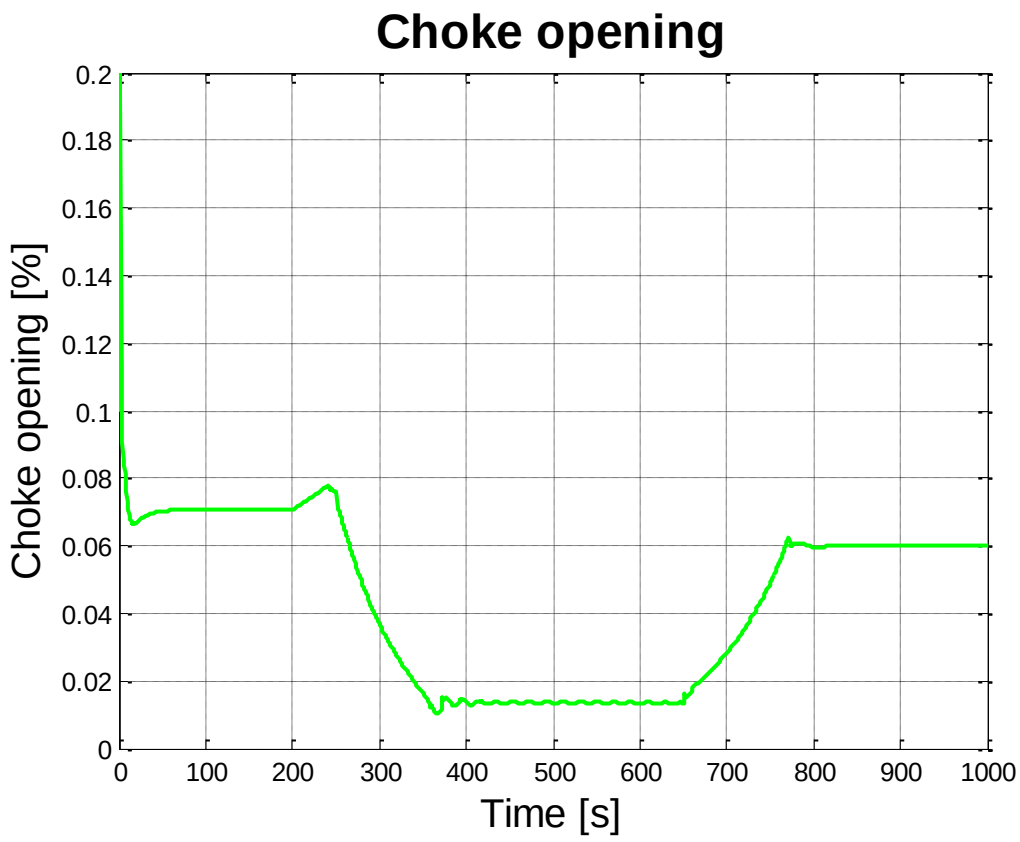

Figure 35: Choke opening with BPP method (modified after [12])

Utilizing of BPP technique in MPD when making a connection.

The fig. 36 details the BPP method in MPD system of making a connection. The system shows how much the backpressure pump rate should increase as the main rig pump rate decreases.

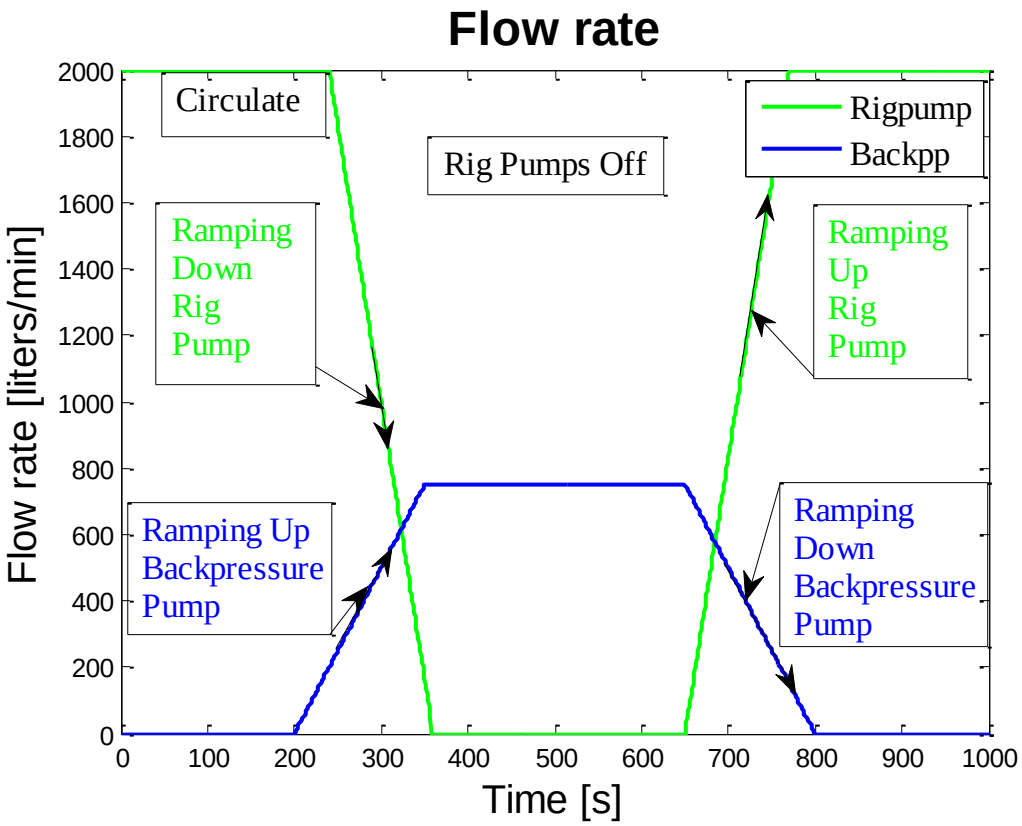

Figure 36: Flow rate with BPP method (modified after [12] [14])

In the case study 2, incompressible drilling fluid was selected. The pressure fluctuations are relatively high. However, the pressure spikes caused by ramping pumps up and down which show in the BHP figure will become even more obvious when drilling with compressible fluid. [14]

7.4.2 Conclusions

With pressure spikes equal to 6.4 bar during ramping down the rig pump may indicate the controller is not properly tuned. The PI control performance is not fully satisfied. The commonly accepted deviation is ± 5 bar. It should be a lesson learned.

References

1. Kårstad, E., *Time-dependent temperature behaviour in rock and borehole*. 1999, Høgskolen i Stavanger: Stavanger.
2. Elliott, D., et al. *Managed Pressure Drilling Erases the Lines*. 2011 [cited 2015 9th of June]; Available from: http://www.slb.com/services/miswaco/services/~/media/Files/resources/oilfield_review/ors11/spr11/managed_pressure.ashx.
3. Hannegan, D.M., *Variations of Managed-Pressure Drilling Currently Practiced:Offshore Case Studies*. Offshore Technology Conference.
4. Onifade, J., et al., *Managed Pressure Drilling System Provided Value to Offshore Drilling Operation*. Society of Petroleum Engineers.
5. SWACO, M.-I. and Schlumberger. *8068/8068-G Rotating Control Device*. 2013 [cited 2015 9th of June]; Available from: http://www.slb.com/~/media/Files/miswaco/product_sheets/mpdubd_model_8068_ps.pdf.
6. Management, E.P. *Micro Motion Coriolis meters accurately detect and quantify wellbore ballooning*. 2013 [cited 2015 9th of June]; Available from: http://www2.emersonprocess.com/siteadmincenter/PM%20Micro%20Motion%20Documents/Drilling-Detection-Wellbore-Ballooning-AN-001785.pdf.
7. SWACO, M.-I. and Schlumberger. *Flat Design MPD manifolds*. [cited 2015 9th of June]; Available from: http://www.slb.com/~/media/Files/miswaco/brochures/choke_manifolds_brochure.pdf.
8. Shelton, J., J.R. Smith, and A. Gupta, *Experimental Evaluation of Separation Methods for a Riser Dilution Approach to Dual Density Drilling.* Journal of Energy Resources Technology, 2011. **133**(3): p. 031501-031501.
9. Karafyllis, I. [cited 2015 9th of June]; Available from: http://www.math.ntua.gr/~iasonkar/.
10. Wikipedia. *PID controller*. [cited 2015 9th of June]; Available from: http://en.wikipedia.org/wiki/PID_controller.
11. Nygaard, G. and J.-M. Godhavn, *Automated Drilling Operation*. 2013, University of Stavanger,Norwegian University of Science and Technology.
12. Østensjø, G.H. and K.L. Syvertsen, *Automated Managed Pressure Drilling*, in *Faculty of Science and Technology*. 2015, University of Stavanger.
13. Kaasa, G.-O., et al., *Intelligent Estimation of Downhole Pressure Using Simplified Hydraulic Model*. Society of Petroleum Engineers.
14. Johnson, R.L., et al., *Field Demonstration of a New Method for Making Drill-Pipe Connections during Managed-Pressure Drilling Operations*. Society of Petroleum Engineers.
15. Kårstad, E. and B.S. Aadnoy, *Analysis of Temperature Measurements during Drilling*. Society of Petroleum Engineers.
16. Kabir, C.S., et al., *Determining Circulating Fluid Temperature in Drilling, Workover, and Well Control Operations.*
17. Holmes, C.S. and S.C. Swift, *Calculation of Circulating Mud Temperatures.*

18. Godhavn, J.-M., *Control Requirements for Automatic Managed Pressure Drilling System.*
19. Veeningen, D.M. and R. Adsit, *Supplementing Downhole Information to Enhance MPD and UBD Operations*. Society of Petroleum Engineers.
20. Hannegan, D.M., *Case Studies-Offshore Managed Pressure Drilling*. Society of Petroleum Engineers.
21. Nauduri, A.S.S., G.H. Medley, and J.J. Schubert, *MPD: Beyond Narrow Pressure Windows*. Society of Petroleum Engineers.
22. Bennion, D.B., et al., *Underbalanced Drilling, Praises and Perils*. Society of Petroleum Engineers.
23. Finley, D.B., et al., *Reservoir Knowledge and Drilling-Benefits Comparison for Underbalanced and Managed Pressure Drilling Operations*. Society of Petroleum Engineers.
24. van Riet, E.J., D. Reitsma, and B. Vandecraen, *Development and Testing of a Fully Automated System to Accurately Control Downhole Pressure During Drilling Operations*. Society of Petroleum Engineers.
25. Hannegan, D.M. and K. Fisher, *Managed Pressure Drilling in Marine Environments*. International Petroleum Technology Conference.
26. Fredericks, P.D., L. Smith, and K.J. Moreau, *ECD Management and Pore Pressure Determination with MPD Improves Efficiency in GOM Well*. Society of Petroleum Engineers.
27. Hannegan, D. and A. Mahmood, *Offshore Well Integrity Management with MPD Tools and Technology*. Offshore Technology Conference.
28. Cantu, J.A., J. May, and J. Shelton, *Using Rotating Control Devices Safely in Today's Managed Pressure and Underbalanced Drilling Operations*. Society of Petroleum Engineers.
29. Belayneh, M.A., *Lecture notes, New drilling technology, Course: PET 525*. Spring 2014.
30. Arnone, M.A. and P. Vieira, *Drilling Wells With Narrow Operating Windows Applying the MPD Constant Bottom Hole Pressure Technology—How Much the Temperature and Pressure Affects the Operation's Design*. Society of Petroleum Engineers.
31. Rehm, B. and C. International Association of Drilling, *Managed pressure drilling*. Gulf drilling series. 2008, Houston, Tex: Gulf Publ. Co. Page 2.
32. Montilva, J.C., J.F. Mota, and R.J. Billa, *Onshore US MPD Use by an Operator*. Society of Petroleum Engineers.
33. Purwagautama, G., et al., *MPD Application With CBHP Technique in Horizontal Well Drilling for the Development of an HPHT and Sour-Environment Gas Field: A Case History*. Society of Petroleum Engineers.
34. Haugen, F., *Basic dynamics and control*. [2nd ed.]. ed. 2010, Skien: TechTeach.
35. Wikipedia. *Control theory*. 2014 [cited 2015 13th of June]; Available from: http://en.wikipedia.org/wiki/Control_theory.
36. Åstrøm, K.J. *Control System Design Lecture notes for ME 155A*. 2002 [cited 2015 9th of June]; Available from: http://www.cds.caltech.edu/~murray/courses/cds101/fa02/caltech/astrom-ch6.pdf.
37. Wikipedia. *Feed forward (control)*. [cited 2015 13th of June]; Available from: https://en.wikipedia.org/wiki/Feed_forward_(control).
38. Kaasa, G.-O., et al., *Simplified Hydraulics Model Used for Intelligent Estimation of Downhole Pressure for a Managed-Pressure-Drilling Control System.*

39. Rehm, B. and C. International Association of Drilling, *Managed pressure drilling*. Gulf drilling series. 2008, Houston, Tex: Gulf Publ. Co.
40. Sui, D., *Drilling data quality control*, in *Wired Drill Pipe Technology*. 2015: Chinese Control Conference.
41. Isambourg, P., B.T. Anfinsen, and C. Marken, *Volumetric Behavior of Drilling Muds at High Pressure and High Temperature*. Society of Petroleum Engineers.
42. Karstad, E., *Analysis of Ballooning Effects During Drilling of High Pressure High Temperature Wells*. Society of Petroleum Engineers.
43. Nygaard, G., *Advanced drilling*. 2014.
44. Jansen, B., et al., *Automatic Control of Unstable Gas Lifted Wells*. Society of Petroleum Engineers.
45. Fredericks, P.D. and D. Reitsma. *MPD automation addresses drilling challenges in conventional, unconventional resources*. 2006 [cited 2015 10th of June]; Available from: http://www.drillingcontractor.org/dcpi/dc-novdec06/DC_Nov07_fredericks.pdf.
46. Saeed, S., R. Lovorn, and K. Arne Knudsen, *Automated Drilling Systems for MPD C-The Reality*. Society of Petroleum Engineers.
47. Bjorkevoll, K.S., et al., *Successful Use of Real Time Dynamic Flow Modelling to Control a Very Challenging Managed Pressure Drilling Operation in the North Sea*. Society of Petroleum Engineers.
48. Tian, S., G.H. Medley, and R. Stone, *Parametric Analysis of MPD Hydraulics*. Society of Petroleum Engineers.
49. Couturier, Y., et al., *New Automated MPD System Provides a Step Change in Performance with a Streamline Equipment Footprint*. Society of Petroleum Engineers.
50. Godhavn, J.-m. and K.A. Knudsen, *High Performance and Reliability for MPD Control System Ensured by Extensive Testing*. Society of Petroleum Engineers.
51. Wikipedia. *Profibus*. [cited 2015 13th of June]; Available from: no.wikipedia.org/wiki/Profibus.
52. Raymond, L.R., *Temperature Distribution in a Circulating Drilling Fluid.*
53. Wooley, G.R., *Computing Downhole Temperatures in Circulation, Injection, and Production Wells.*
54. Hasan, A.R., C.S. Kabir, and M.M. Ameen, *A Fluid Circulating Temperature Model for Workover Operations.*
55. Guillot, F., J.M. Boisnault, and J.C. Hujeux, *A Cementing Temperature Simulator To Improve Field Practice*. Society of Petroleum Engineers.
56. Cui, L., H. Wang, and Y. Ge, *Detailed Hydraulic Simulation of MPD Operation in Narrow Pressure Windows*. Society of Petroleum Engineers.
57. Holman, J.P., *Heat transfer*. 10th ed. ed. McGraw-Hill series in mechanical engineering. 2010, Boston, Mass: McGraw-Hill.
58. Zolotukhin, A.B., *Analytical Definition Of The Overall Heat Transfer Coefficient*. Society of Petroleum Engineers.
59. Demirdal, B., et al., *Drilling Fluids Rheological and Volumetric Characterization Under Downhole Conditions*. Society of Petroleum Engineers.
60. McMordie, W.C., Jr., R.G. Bland, and J.M. Hauser, *Effect of Temperature and Pressure on the Density of Drilling Fluids*. Society of Petroleum Engineers.
61. Patel, B., B. Grayson, and H. Gans, *Optimized Unconventional Shale Development With MPD Techniques*. Society of Petroleum Engineers.

62. Rommetveit, R. and K.S. Bjorkevoll, *Temperature and Pressure Effects on Drilling Fluid Rheology and ECD in Very Deep Wells*. Society of Petroleum Engineers.

Appendix

Appendix A:

Effect of inlet mud temperature on temperature and density behaviors for a shallower well

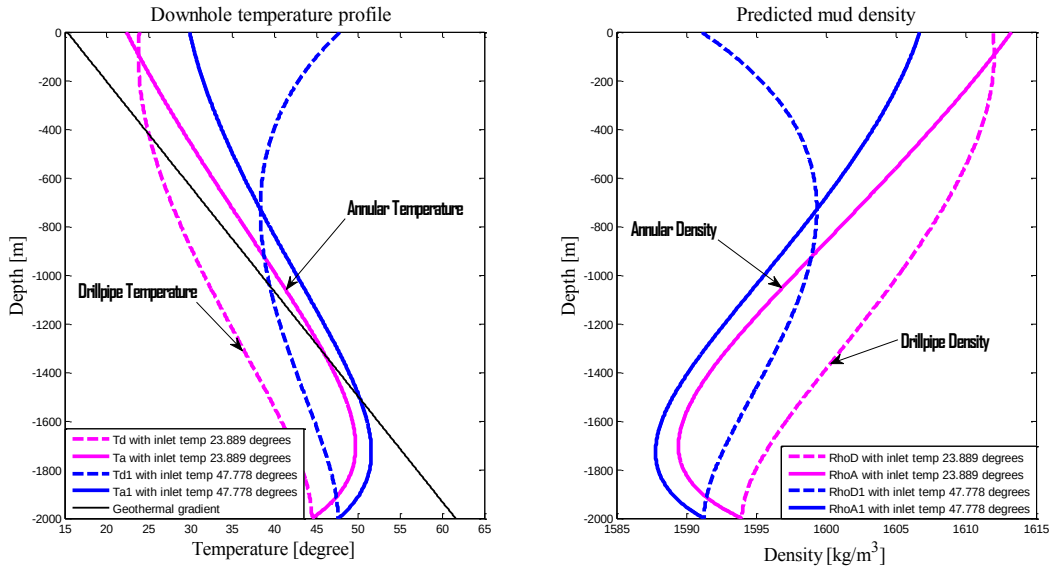

Figure 37 effect of inlet mud temperature on temperature and density behaviors for a 2000meters well

Appendix B

MatLab codes used for plotting of figure 13:

```
clear all;
close all;
dens0=1.6*.01;
temp0=20;
alpha = -5.4489*10^-4;
beta = 1.5449*10^4;
pres0 = 9.3201;

dens_1 = [];
dens_2 = [];
dens_3 = [];
dens_4 = [];
dens_5 = [];
dens_6 = [];
dens_7 = [];
dens_8 = [];
```

```
dens_9 = [];
pres=490.528;

for z = 1:1:pres;
    dens1 = dens0 + (dens0/beta)*(z-pres0)-dens0*alpha*(4-temp0);
    dens2= dens0 + (dens0/beta)*(z-pres0)-dens0*alpha*(20-temp0);
    dens3 = dens0 + (dens0/beta)*(z-pres0)-dens0*alpha*(50-temp0);
    dens4= dens0 + (dens0/beta)*(z-pres0)-dens0*alpha*(75-temp0);
    dens5= dens0 + (dens0/beta)*(z-pres0)-dens0*alpha*(100-temp0);
    dens6= dens0 + (dens0/beta)*(z-pres0)-dens0*alpha*(125-temp0);
    dens7= dens0 + (dens0/beta)*(z-pres0)-dens0*alpha*(150-temp0);
    dens8= dens0 + (dens0/beta)*(z-pres0)-dens0*alpha*(175-temp0);
    dens9= dens0 + (dens0/beta)*(z-pres0)-dens0*alpha*(200-temp0);

    dens_1 = [dens_1;dens1];
    dens_2 = [dens_2;dens2];
    dens_3 = [dens_3;dens3];
    dens_4 = [dens_4;dens4];
    dens_5 = [dens_5;dens5];
    dens_6 = [dens_6;dens6];
    dens_7 = [dens_7;dens7];
    dens_8 = [dens_8;dens8];
    dens_9 = [dens_9;dens9];
 end
figure;
plot(
1:1:pres,dens_1,1:1:pres,dens_2,1:1:pres,dens_3,1:1:pres,dens_4,1:1:pres,dens_
5,1:1:pres,dens_6,1:1:pres,dens_7,1:1:pres,dens_8, 1:1:pres,dens_9);
%plot(pres,dens_1,'r',pres,dens_2,'b',pres,dens_3,'g',pres,dens_4,'b');
legend('linearized with T=4','linearized withT=20','linearized with
T=50','linearized with T=75','linearized with T=100','linearized with
T=125','linearized with T=150','linearized with T=175','linearized with
T=200');
title('True density & linearized density
profile','fontsize',18,'FontName','Times');
xlabel('Pressure[bar]');
ylabel('Density[kg/m^3]');
hold on;
```

Appendix B

Data used to plot figure 14:

```
function cost=pdt(x,para)

t=para.temp;
p=para.pres;
d=para.dens;
y=[];

for i=1:length(t)
    for j=1:length(p)
```

```
        temp=x(1)+x(2)*t(i)+x(3)*p(j)-d(j,i);
        y=[y;temp];
    end
end
cost=sum(abs(y));
```

Data used to plot figure 14:

```
function [c,ceq]=constraint_x(x,para)

ceq=[];
c(1)=-x(3);
```

Data used to plot figure 14:

```
temp=[4,20,50,75,100,125,150,175,200];
pres=[1,14.790,42.230,69.940,90.632,118.211,145.790,173.369,200.948,228.527,25
6.106,311.264,366.422,435.370,490.528];
dens=.01*[
1.61406  1.60169  1.57651  1.55393  1.53015  1.5053   1.47945  1.45256 1.42452
1.61508  1.60278  1.57778  1.55536  1.53174  1.50707  1.48141  1.45472 1.42688
1.61709  1.60495  1.58029  1.55819  1.5349   1.51059  1.48528  1.45897 1.43154
1.61908  1.6071   1.58278  1.56098  1.53802  1.51404  1.4891   1.46316 1.43612
1.62056  1.6087   1.58462  1.56305  1.54033  1.5166   1.49192  1.46625 1.4395
1.62253  1.61082  1.58706  1.56578  1.54337  1.51997  1.49563  1.47032 1.44394
1.62448  1.61291  1.58946  1.56847  1.54637  1.52328  1.49928  1.47432 1.44831
1.62641  1.61499  1.59184  1.57112  1.54932  1.52655  1.50286  1.47824 1.4526
1.62833  1.61704  1.59419  1.57374  1.55223  1.52976  1.50639  1.48211 1.45681
1.63022  1.61908  1.59651  1.57633  1.55509  1.53292  1.50986  1.4859  1.46094
1.63211  1.62109  1.5988   1.57888  1.55792  1.53603  1.51327  1.48962 1.465
1.63583  1.62506  1.6033   1.58387  1.56344  1.5421   1.51992  1.49687 1.47289
1.63948  1.62894  1.60769  1.58872  1.56878  1.54797  1.52634  1.50386 1.48048
1.64396  1.63369  1.61302  1.5946   1.57524  1.55503  1.53403  1.51223 1.48956
1.64747  1.6374   1.61716  1.59914  1.58021  1.56046  1.53994  1.51863 1.4965
 ];

 dens0=1.6*.01;
 temp0=20;

 para.temp=temp;
 para.pres=pres;
 para.dens=dens;
 x0=[1,1,1];

 opt=fmincon('pdt',x0,[],[],[],[],[],[],'constraint_x',[],para);

 %***************rho=a+bP+cT********************
a=opt(1);
b=opt(3);
```

```
c=opt(2);

beta=dens0/b;
alpha=c/dens0;
pres0=(dens0-c*temp0-a)/b;
 %***************rho=a+bP+cT*********************


function [c,ceq]=constraint_x(x,para)

ceq=[];
c(1)=-x(3);
```

Appendix C

MatLab codes used for plotting of figure 19.

```
clear all;
clc;
close all;

%% well description
%%Twb wellbore interface temperature
%%Ta  annular fluid temperature
%%Td  ubular fluid temperature
%%Tf virgin formation temperature
%%q_ad conductive heat transfer through the drill string
%%q_f  conductive heat transfer between the annulus and the formation
%%q_d  conductive heat in the drill string at z
%%Ud [W/m^2 degree] is overall heat-transfer coefficient related to
drillstring
%%Ua [W/m^2 degree] is overall heat-transfer coefficient related to annulus
Ua=250;
Ud=125;
t=1; %circulation time
rho_m=1198.264;%%[kg/m^3]  mud density
qcirculate = 0.013249; %[m^3/s]   % or 47.6964m^3/hr
w = qcirculate*rho_m; %[kg/s] mass flow rate
depth=4800;%%[m]  vertical well depth
rd=0.08414;%%  3.3125in [meter] drill pipe radius
rc= 0.1064;%% 4.1875in  [meter] formation radius

gG=0.023148;%%[degree/m]  geothermal gradient
Tsf=15.278;%%[degree]  surface earth temperature
Tin=23.889;%23.889;%%[degree]  inlet fluid temperature

Cfl=1676;%%[J/(kg degree)]  mud specific heat
cf=838;%%[J/(kg degree)]  formation specific heat
```

```
kf=2.250;%%[W/(m degree)]  formation thermal conductivity
Kfl=1.730;%%[W/(m degree)]  mud thermal conductivity
rho_f = 2643;%%[kg/m^3]
%% related parameters
alpha_h=kf/(rho_f*cf);%%(2.3) [m^2/s]  thermal diffusivity

tD=(alpha_h*t/rc^2)*3600;%%(2.4)  dimensionless time
%%Forward circulation-fluid flow down the drill string
%%chose z to be positive in the downward direction,and fluid is flowing
%%down the drillstring and up through the annulus%%f(tD) is dimensionless time
function
if 10^-10 <= tD <=1.5
    f_tD= (1.1281*sqrt(tD))*(1-0.3*sqrt(tD));%%(2.2a)
elseif tD>1.5
    f_tD=(0.4063+0.5*log(tD))*(1+0.6/tD);%%(2.2b)
end

T_d=[];
T_a=[];
T_f=[];
rho_d=[];
rho_a=[];
for z=0:1:depth;
     A = (w*Cfl/(2*pi*rc*Ua))*(1+(rc*Ua*f_tD)/kf);%%(2.12a)
     B = (w*Cfl)/(2*pi*rd*Ud);%%(2.12b)
     lambda1 = 1/(2*A)*(1-sqrt(1+4*A/B));%%(2.16)
     lambda2 = 1/(2*A)*(1+sqrt(1+4*A/B));%%(2.17)

     alpha=-((Tin+B*gG-
Tsf)*lambda2*exp(lambda2*depth)+gG)/(lambda1*exp(lambda1*depth)-
lambda2*exp(lambda2*depth));%%(2.18)
     beta=((Tin+B*gG-Tsf)*lambda1*exp(lambda1*depth)+gG) /
(lambda1*exp(lambda1*depth)-lambda2*exp(lambda2*depth));%%(2.19)

     Tf =Tsf+gG*z;

     T_0 = 20;%[degree] ADDED REFERENCE POINT FOR THE LINEARIZATION
     P_0 = 9.32e5;% [pa] ADDED REFERENCE POINT FOR THE LINEARIZATION
     rho_0 = 1600;%[kg/m^3] ADDED REFERENCE POINT FOR THE LINEARIZATION
     alpha_0 = 5.45*10^-4; %ADDED cubical expansion coefficient of the liquid
     beta_0 = 1.55e9; %ADDED isothermal bulk modulus of the liquid [pa] or
15500bar
     g=9.81;
     p_atmospheric =1.013e5;%[pa] eller 101.325;[kpa]
     P = (rho_0*g*depth+p_atmospheric)/2;

     Td = alpha*exp(lambda1*z)+ beta*exp(lambda2*z)+gG*z-B*gG+Tsf;%%(2.14)
     Ta = (1+lambda1*B)*
alpha*exp(lambda1*z)+(1+lambda2*B)*beta*exp(lambda2*z)+gG*z+Tsf;%%(2.15)

     T_f = [T_f;Tf];
     rhod = rho_0+(rho_0/beta_0)*(P-P_0)-rho_0*alpha_0*(Td-T_0);
     rhoa = rho_0+(rho_0/beta_0)*(P-P_0)-rho_0*alpha_0*(Ta-T_0);
```

```
      T_d = [T_d;Td];
      T_a = [T_a;Ta];
      rho_d=[rho_d;rhod];
      rho_a=[rho_a;rhoa];
end
figure;
subplot(1,2,1);
plot(T_d,0:-1:-depth,'r',T_a,0:-1:-depth,'b',T_f,0:-1:-depth,'k');
title('Downhole temperature profile ','fontsize',16,'FontName','Times');
xlabel('Temperature [degree]','fontsize',15,'FontName','Times');
ylabel('Depth [m]','fontsize',15,'FontName','Times');
grid on
subplot(1,2,2);
plot(rho_d,0:-1:-depth,'r',rho_a,0:-1:-depth,'b');
title('Predicted mud density','fontsize',16,'FontName','Times');
xlabel('Density [kg/m^3]','fontsize',15,'FontName','Times');
ylabel('Depth [m]','fontsize',15,'FontName','Times');
grid on
```